# Atmospheric measurements of Δ17O in CO2 in Göttingen, Germany reveal a seasonal cycle driven by biospheric uptake

Hofmann, M. E. G.; Horvath, B.; Schneider, L.; Peters, W.; Schützenmeister, K.; Pack, A.

*Published in:*
Geochimica et Cosmochimica Acta

*DOI:*
10.1016/j.gca.2016.11.019



*Publication date:*
2017

Available online at www.sciencedirect.com

ScienceDirect

Geochimica et Cosmochimica Acta 199 (2017) 143–163

Geochimica et Cosmochimica Acta

www.elsevier.com/locate/gca

# Atmospheric measurements of $\Delta^{17}O$ in $CO_2$ in Göttingen, Germany reveal a seasonal cycle driven by biospheric uptake

M.E.G. Hofmann [a,b,*], B. Horváth [a,1], L. Schneider [c,2], W. Peters [c,d], K. Schützenmeister [e,3], A. Pack [a]

[a] Isotope Geology Section, University of Göttingen, Germany
[b] Institute for Marine and Atmospheric Research (IMAU), Utrecht University, The Netherlands
[c] Meteorology and Air Quality Section, Wageningen University, The Netherlands
[d] Centre for Isotope Research, University of Groningen, The Netherlands
[e] Department of Landscape Ecology, University of Göttingen, Germany

Received 31 August 2015; accepted in revised form 12 November 2016; available online 20 November 2016

**Abstract**

The triple oxygen isotope composition of tropospheric $CO_2$ might be a promising new tracer for terrestrial gross carbon fluxes. This notion is based on global box modeling of its abundance, and on highly challenging and therefore very sparse measurements of $^{16}O$, $^{17}O$ and $^{18}O$ in $CO_2$ in the lower atmosphere. Here, we present additional high-precision triple oxygen isotope measurements of ambient air $CO_2$ sampled in Göttingen (NW Germany) over the course of 2 years and of two air samples taken on top of the Brocken Mountain (1140 m, NW Germany). Göttingen differs from other locations where $\Delta^{17}O$ was measured by its proximity to both urban sources of $CO_2$, and to extensive uptake of $CO_2$ by vegetation. In our analysis, we specifically try to discern this latter influence on our measurements, and to distinguish it from other known sources of variation in $\Delta^{17}O$.

Our triple oxygen isotope data are reported as $\Delta^{17}O$ values relative to a $CO_2$-water equilibration line with $\Delta^{17}O = \ln(\delta^{17}O + 1) - 0.5229 \times \ln(\delta^{18}O + 1)$. We report an average of -0.02 ± 0.05‰ (SD) in the first year and -0.12 ± 0.04‰ (SD) in the second year of our measurements. This year-to-year difference is higher than expected based on other available $\Delta^{17}O$ records, but careful scrutiny of our measurement approach did not reveal obvious analytical biases, leaving this aspect of our record unexplained. After removing the year-to-year trend, our time series shows a statistically robust seasonal cycle with maximum values in June/July and an amplitude (peak-to-trough) of 0.13 ± 0.02‰. We compare our observational data to a revised triple oxygen isotope mass balance "box" model of tropospheric $CO_2$ where we reconcile both $^{18}O/^{16}O$ and $^{17}O/^{16}O$ fractionation processes. We also compare them to Göttingen-specific output from a three-dimensional transport model simulation of $\Delta^{17}O$ in $CO_2$ performed with the Tracer Model 5 (TM5). Both the modeled isofluxes at the surface, and the modeled stratospheric, fossil, and biospheric $\Delta^{17}O$ components in the atmosphere at Göttingen confirm that the observed seasonal cycle in $\Delta^{17}O$ is driven primarily by the seasonal cycle of gross primary productivity (GPP), and that the seasonal variations in both stratospheric transport and fossil fuel emissions play a minor role at our location. Our results therefore strengthen earlier

* Corresponding author at: Princetonplein 5, 3584CC Utrecht, The Netherlands.
*E-mail addresses:* m.e.g.hofmann@uu.nl (M.E.G. Hofmann), horvath@imprint-analytics.at (B. Horváth), linda.schneider@kit.edu (L. Schneider), wouter.peters@wur.nl (W. Peters), schuetzenmeister@uni-landau.de (K. Schützenmeister), apack@gwdg.de (A. Pack).
[1] Now at: Imprint Analytics, Austria.
[2] Now at: Institute of Meteorology and Climate Research, Karlsruhe Institute of Technology, Germany.
[3] Now at: Geoecology and Physical Geography Section, University of Koblenz-Landau, Germany.

http://dx.doi.org/10.1016/j.gca.2016.11.019

suggestions that GPP is reflected in $\Delta^{17}O$, and call for more seasonally resolved measurements at continental locations like Göttingen.


*Keywords:* Triple oxygen isotopes; $^{17}O$; Carbon dioxide; Terrestrial gross primary production; Troposphere; $\Delta^{17}O$; 3D transport model; TM5

## 1. INTRODUCTION

The stable isotope composition of atmospheric carbon dioxide ($CO_2$) gives insight into the magnitude of carbon fluxes between the atmosphere, biosphere and ocean. The carbon isotope ratio allows to quantify the oceanic carbon dioxide uptake due to a distinct discrimination of $^{13}C/^{12}C$ during $CO_2$ uptake by the ocean and by plants (Ciais et al., 1995). The oxygen isotope ratio $^{18}O/^{16}O$ of carbon dioxide has been explored extensively as a tracer of gross carbon fluxes between the atmosphere and biosphere (Farquhar et al., 1993; Ciais et al., 1997; Cuntz et al., 2003a,b; Welp et al., 2011).

Hoag et al. (2005) were the first to set-up a two-box mass balance model for the triple oxygen isotope abundance of tropospheric $CO_2$ and suggested that high precision measurements of tropospheric $CO_2$ (denoted as $\Delta^{17}O$, see Section 2.1 for definition) can provide further constraints on terrestrial gross carbon fluxes. The idea is based on the fact that the $\Delta^{17}O$ value of tropospheric $CO_2$ is controlled by the inflow of mass-independently fractionated $CO_2$ from the stratosphere (Thiemens et al., 1995; Lämmerzahl et al., 2002; Boering et al., 2004; Kawagucci et al., 2008; Wiegel et al., 2013) and mass-dependently fractionated $CO_2$ from the biosphere. The authors argue that the triple oxygen isotope composition of tropospheric $CO_2$ should be a more direct tracer of gross primary productivity than variations in $^{18}O/^{16}O$.

The analysis of the triple oxygen isotope composition of tropospheric $CO_2$ has long been limited by the measurement precision of $\Delta^{17}O$ in $CO_2$. In recent years, several methods for high precision measurements of $\Delta^{17}O$ in $CO_2$ have been developed (Hofmann and Pack, 2010; Barkan and Luz, 2012; Mahata et al., 2012, 2013; Passey et al., 2014) and first high precision measurements of $\Delta^{17}O$ of tropospheric $CO_2$ have been carried out (Barkan and Luz, 2012; Thiemens et al., 2014; Liang and Mahata, 2015). Thiemens et al. (2014) report a record of $\Delta^{17}O$ values of tropospheric $CO_2$ sampled in La Jolla, California (USA) between 1991 and 2000 and suggest that an observed drop in $\Delta^{17}O$ in 1997 might be related to an enhanced global primary productivity. They also conclude that the mean triple oxygen isotope composition of near-surface $CO_2$ indeed reveals a stratospheric component. Liang and Mahata (2015) suggest that variations in the triple oxygen isotope composition of near-surface $CO_2$ sampled in Taiwan result from downwelling events of stratospheric $CO_2$. However, the quantitative interpretation of temporal and regional variations in $\Delta^{17}O$ of $CO_2$ is hindered by the lack of a more comprehensive atmospheric model for the triple oxygen isotope composition of tropospheric $CO_2$.

Here, we present a two-year time series of triple oxygen isotope measurements of carbon dioxide sampled in Göttingen, a medium-sized town located in the center of Germany, and triple oxygen isotope data of $CO_2$ sampled on top of the nearby Brocken Mountain. In contrast to the previous sampling sites for $\Delta^{17}O$ analysis of $CO_2$, we suspect that local carbon dioxide fluxes are dominated by seasonal variations in biospheric activity.

We set up a revised global mass balance "box" model for the triple oxygen isotope composition of tropospheric $CO_2$, where we reconcile the assumptions for $^{18}O/^{16}O$ and $^{17}O/^{16}O$ fractionation of atmospheric $CO_2$: (i) we implement the experimental results for the exponent $\theta$ for $CO_2$-water equilibrium (Hofmann et al., 2012; Barkan and Luz, 2012), (ii) we take into account that the main water reservoirs that exchange with atmospheric $CO_2$ (ocean, soil and leaf water) have a distinct triple oxygen isotope signature (Landais et al., 2006; Luz and Barkan, 2010) and (iii) we assume that $CO_2$ sinks can also fractionate the triple oxygen isotope composition.

In a separate effort, this same model formulation was extended into three-dimensional space using a combination of the Tracer Transport Model 5 and the SiBCASA terrestrial biosphere model for $CO_2$ exchange. We use the temporal variation in the triple oxygen isotope composition of tropospheric $CO_2$ in a $6 \times 4°$ grid cell surrounding our sampling location Göttingen to quantitatively evaluate temporal variations in $\Delta^{17}O$ of $CO_2$ at our sampling location.

## 2. EXPERIMENTAL METHODS AND MATERIALS

### 2.1. Triple oxygen isotope notation

Oxygen isotope ratios ($^{17}O/^{16}O$ and $^{18}O/^{16}O$) are traditionally reported as $\delta$-values relative to VSMOW:

$$\delta^{17}O = \frac{(^{17}O/^{16}O)_{sample}}{(^{17}O/^{16}O)_{VSMOW}} - 1 \quad (2\text{-}1)$$

and

$$\delta^{18}O = \frac{(^{18}O/^{16}O)_{sample}}{(^{18}O/^{16}O)_{VSMOW}} - 1 \quad (2\text{-}2)$$

Small variations in the triple oxygen isotope composition are reported as deviations from a mass-dependent reference line in a triple oxygen isotope plot with logarithmic $\delta$-coordinates (Hulston and Thode, 1965; Miller, 2002; Young et al., 2002):

$$\Delta^{17}O_{RL} = \ln(\delta^{17}O + 1) - \lambda_{RL} \times \ln(\delta^{18}O + 1) - \gamma_{RL} \quad (2\text{-}3)$$

Different reference lines (RL) are currently being used in the literature to report variations in the triple oxygen isotope abundance: (i) the so-called terrestrial fractionation line defined by the isotopic composition of rocks and minerals with $\lambda_{RL} = 0.525$ (Hofmann and Pack, 2010; Hofmann et al., 2012), (ii) the meteoric water line defined by the isotopic composition of precipitation water with a slope of 0.528 (Landais et al., 2008), (iii) a VSMOW-SLAP reference line with again a slope of 0.528 that is tied to these two international water standards (Barkan and Luz, 2012), (iv) a slope of 0.516 that was selected empirically by Boering et al. (2004) based on stratospheric $CO_2$ measurements to represent the isotopic composition of tropospheric $CO_2$ entering the stratosphere and this slope was also adopted by others (Hoag et al., 2005; Liang and Mahata, 2015), (v) a slope of 0.5305 that corresponds to the equilibrium end-member for isotope fractionation at high temperatures (Pack and Herwartz, 2014; Herwartz et al., 2014; Gehler et al., 2016), (vi) and a $CO_2$-water equilibration line with a slope of 0.522 (Horváth et al., 2012; Thiemens et al., 2014) based on the experimental findings from Hofmann et al. (2012). Although no consensus has yet been reached on a common reference line, it is important to note that the choice of reference line is somewhat arbitrary since $\Delta^{17}O$ is not a measured quantity but inferred from $\delta^{17}O$ and $\delta^{18}O$ (Kaiser, 2008; Pack and Herwartz, 2014). In this study, we take a $CO_2$-water equilibration line as reference line with a slope $\lambda_{RL} = 0.5229$ based on the refined $CO_2$-water equilibrium fractionation factor (Barkan and Luz, 2012) and zero intercept, e.g. $\gamma_{RL} = 0‰$. We chose this slope because the equilibration between $CO_2$ and water is the dominant process controlling the abundance of $\Delta^{17}O$ in tropospheric $CO_2$ and the zero intercept was chosen for simplicity. The logarithmic $\delta$-values are abbreviated as $\delta$'-values with $\delta'^{17}O = \ln(\delta^{17}O + 1)$ and $\delta'^{18}O = \ln(\delta^{18}O + 1)$. For the $^{18}O/^{16}O$ mass balance calculation, all oxygen isotope ratios are reported as $\delta^{18}O$ values.

### 2.2. Sampling of tropospheric $CO_2$ and isotope analysis

We sampled ambient air $CO_2$ in two-week intervals from June 2010 to August 2012 from the fourth floor of the Geoscience Department in Göttingen, Germany. The department is situated at the outskirts of the medium-sized town Göttingen with moderate traffic density (130,000 inhabitants, 51.5569°N, 9.9468°E).

Additionally, we sampled three air samples on top of the nearby Brocken Mountain, the highest peak of the Harz Mountain range with an elevation of about 1140 m (51.7987°N, 10.6185°E). The Mt. Brocken is situated in a low populated national park with smaller towns (5000–50,000 inhabitants) at a distance of 5–30 km. The mountain range stands out of the surrounding lowlands and it is mostly exposed to low tropospheric winds from west/southwest. In the prevailing wind direction, major cities (>200,000 inhabitants) are at a distance of at least 100 km. The Brocken air was sampled on 2nd and 28th March and 17th July 2012 in order to check if the air samples from Göttingen were significantly affected by elevated anthropogenic $CO_2$ influx (Horváth et al., 2012) or local $CO_2$ sources from the biosphere. The $\delta^{18}O$ value of the $CO_2$ sampled on the 17th July 2012 deviated by about 1.9‰ from the seasonal cycle observed in Göttingen (see Section 3.3) indicating that this sample $CO_2$ might have been affected by re-equilibration with water during sampling or subsequent gas handling. Therefore, it had to be discarded.

In Göttingen, the $CO_2$ was directly extracted from ambient air using a Russian doll type cryogenic trap with borosilicateglass filters (Brenninkmeijer, 1991; Brenninkmeijer and Röckmann, 1996). A tube was installed at the building so that ambient air was collected with 1–2 m distance to the building. First, the ambient air passed through magnesium perchlorate, $Mg(ClO_4)_2$, to remove water vapor. Then, the $CO_2$ was separated from all non-condensable gases by means of the cryogenic trap at a flow rate of 2–3 L/min. In order to analyze the $\Delta^{17}O$ of $CO_2$ we use a $CO_2$-$CeO_2$ equilibration technique which requires at least 3.5 mmol of $CO_2$ (corresponding to about 400 L of ambient air at STP) (Hofmann and Pack, 2010; Hofmann et al., 2012; Horváth et al., 2012).

Subsequent to the collection of $CO_2$ in the Russian doll type cryogenic trap, the cold trap is slowly warmed to room temperature. Simultaneously, a second trap is held at −70 °C (with a mixture of liquid nitrogen and ethanol) to hold back remaining water vapor. Next, the $CO_2$ gas is exposed for about 30 min to $P_2O_5$ for final drying. A subsample of the $CO_2$ (~50 µmol) is separated for conventional $\delta^{13}C$ and $\delta^{18}O$ analyses. The remaining $CO_2$ sample is then immediately transferred to the $CO_2$-$CeO_2$ equilibration apparatus, so that no storage of the sample $CO_2$ becomes necessary.

Air sampling on top of the Brocken Mountain was carried out with an oil-free, high-pressure compressor from Rix Industries with a gas engine drive (model SA-3G). The air inlet was held at about 4 m above ground. The air stream passed through two $Mg(ClO_4)_2$ units in order to effectively remove water vapor. Before entering the compressor, the flow rate was controlled with a mass flow controller, which was set to 2–3 L/min. The dried air was compressed into a 5 L pressure cylinder, which was filled up to 100 bar. A 3 m long exhaust pipe was attached to the compressor to ensure that the exhaust fumes were directed away from the air inlet system. Additionally, the compressor and the exhaust pipe were placed downwind so that the air samples were not contaminated with exhaust gases. The $CO_2$ extraction from the compressed air and the sample preparation was carried out analog to the procedure described above.

The $\delta^{18}O$ and $\delta^{13}C$ analyses of $CO_2$ were carried out on a Finnigan Delta plus mass spectrometer. The stable isotope values were standardized by comparison with $CO_2$ generated by phosphoric acid decomposition of NBS-19 ($\delta^{18}O_{VSMOW} = +28.65‰$, $\delta^{13}C_{VPDB} = +1.95‰$). The carbonate was reacted at 70 °C and the acid fractionation factor for calcite $\alpha_{CO2\text{-}calcite} = 1.00871$ (Kim et al., 2007) was used. The mass spectrometric uncertainty in $\delta^{18}O$ and $\delta^{13}C$ is in the range of ±0.03‰ (1$\sigma$, SD). The $\delta^{18}O$ and $\delta^{13}C$ uncertainty for repeated $CO_2$ extraction from air is in the range of 0.2‰ and 0.1‰, respectively. The

uncertainty in $\delta^{18}O$ is caused by mass-dependent fractionation during the $CO_2$ extraction procedure, i.e. processes with a slope between 0.509 and 0.53. Therefore, the effect on $\Delta^{17}O$ is smaller than 0.003‰ and far lower than the analytical precision for $\Delta^{17}O$ (see below).

Cryogenic $CO_2$ extractions from air do not allow separating $CO_2$ from $N_2O$, and therefore, all $CO_2$ isotope measurements have to be corrected for $N_2O$ interferences. We measured $CO_2$ and $N_2O$ concentrations of the air samples with an auto-sample, computer controlled (Probe 64.1, V1.31, Loftfield et al., 1997) gas chromatograph (Shimadzu GC-14B, Tokyo, Japan). $CO_2$ and $N_2O$ were detected by a $^{63}Ni$ electron capture detector. The $\delta^{13}C$ and $\delta^{18}O$ values were corrected for interferences with $N_2O$ according to the procedure described by Assonov et al. (2009): $\delta^{13}C$ data of ambient air $CO_2$ were corrected with $-0.22 \pm 0.03$‰ (SD), $\delta^{18}O$ data of ambient air $CO_2$ were corrected with $-0.29 \pm 0.03$‰ (SD). No $N_2O$ correction is required for $\Delta^{17}O$ analyses of $CO_2$ because the triple oxygen isotope composition is inferred from $O_2$ measurements (see below).

The $\Delta^{17}O$ analyses were carried out using the $CO_2$-$CeO_2$ exchange method (Hofmann and Pack, 2010; Hofmann et al., 2012; Horváth et al., 2012): An excess of $CO_2$ was equilibrated with $CeO_2$ powder at 685 °C, the equilibrated $CeO_2$ fluorinated and the abundance of $\Delta^{17}O$ analyzed on the released $O_2$. Each $CO_2$-equilibrated $CeO_2$ sample was analyzed 3–6 times. For atmospheric samples, the $N_2O/CO_2$ ratio is <0.001 during the $CeO_2$ equilibration process so that the effect of mass-dependently fractionated $N_2O$ on the $\Delta^{17}O$ signature of $CeO_2$ is <0.001‰, i.e. significantly lower than our measurement precision of about 0.025‰. The method was calibrated by producing $CO_2$ with a known triple oxygen isotope composition by combustion of graphite with $O_2$ ($\delta^{18}O_{VSMOW} = 13.473$‰, $\delta^{17}O_{VSMOWVSMOW} = 6.649$‰) that was analyzed relative to VSMOW by E. Barkan (Institute of Earth Sciences, Hebrew University of Jerusalem).

## 3. EXPERIMENTAL RESULTS

### 3.1. Temporal variation in $CO_2$ concentration

The carbon dioxide concentration observed in Göttingen varies between 375 and 475 ppm (Table 1). The seasonal cycle of $CO_2$ concentration shows lower values during summer ($408 \pm 27$ ppm (SD)) and higher during wintertime ($426 \pm 19$ ppm (SD)) (Fig. 1a) as expected at a continental location on the northern hemisphere. During the same period, the $CO_2$ concentration observed at the Meteorological Observatory Hohenpeissenberg (986 m.a.s.l., ca. 500 km south of Göttingen) varies seasonally between 370 and 400 ppm. The Meteorological Observatory Hohenpeissenberg is the closest background station monitoring at the same time the $CO_2$ concentration and the $\delta^{13}C$ and $\delta^{18}O$ values. The $CO_2$ concentration observed in Göttingen is up to 75 ppm higher than at Hohenpeissenberg. The high enrichment in carbon dioxide in Göttingen compared to the background station reflects the enhanced contribution of local carbon dioxide sources from soil respiration and anthropogenic emissions. The two samples from Mt. Brocken that were analyzed in this study fall within the range observed at the Meteorological Observatory Hohenpeissenberg (see Fig. 1a, Table 2).

### 3.2. $\delta^{13}C(CO_2)$ time series data

The $\delta^{13}C$ values varied between −7.8‰ and −11.0‰ (Fig. 1b, Table 1). High $\delta^{13}C$ values were generally observed during summer and low $\delta^{13}C$ values during winter. This reflects the general pattern of the seasonal cycle in the carbon isotope composition: During summer, plants take up more carbon dioxide during photosynthesis and due to the strong fractionation during photosynthetic carbon uptake (Brugnoli et al., 1988; Guy et al., 1993) this leads to an enrichment in $\delta^{13}C$ in atmospheric $CO_2$. In the first year, the $\delta^{13}C$ values show a pronounced seasonal pattern that is in good agreement with the seasonal cycle observed at the Meteorological Observatory Hohenpeissenberg: The amplitude of the seasonal pattern is about 0.45‰ at both locations and the mean value is only slightly shifted by about 0.15‰ towards lower values at Göttingen. In the second year, the $\delta^{13}C$ values show a large scatter and the carbon isotope composition is depleted by up to −3‰ in Göttingen compared to the Hohenpeissenberg observatory.

The elevated $CO_2$ concentrations in Göttingen compared to the background station suggest a higher contribution of respiratory $CO_2$ from the biosphere and/or from anthropogenic emissions. In general, organic matter is depleted in $\delta^{13}C$, and therefore, soil and anthropogenic $CO_2$ should lower the $\delta^{13}C$ value in the Göttingen air samples. The different $\delta^{13}C$ pattern in the first and second year despite a similar pattern in $CO_2$ concentration is unclear (see Supplementary information for Keeling plot). It may be caused by a change in local $CO_2$ sources, in particular anthropogenic $CO_2$ emissions.

The $\delta^{13}C$ values observed at the Mt. Brocken agree with the observations at the atmospheric monitoring station Hohenpeissenberg (Fig. 1b, Table 2).

### 3.3. $\delta^{18}O(CO_2)$ time series data

The $\delta^{18}O$ values show a pronounced seasonal cycle with low values during winter, i.e. October to March ($\delta^{18}O_{VSMOW} = 41.0 \pm 0.5$‰ (SD)), and high values during summer, i.e. April to September ($\delta^{18}O_{VSMOW} = 42.1 \pm 0.7$‰ (SD)), with an average value of $41.7 \pm 0.8$‰ (Fig. 1c, Table 1). This seasonal cycle is mainly controlled by a higher contribution of assimilation fluxes during summer and a higher contribution of respiratory fluxes during winter (see Fig. 3a). The amplitude and the mean value of the fitted sinusoidal $\delta^{18}O$ function are $0.9 \pm 0.1$‰ and $41.5 \pm 0.1$‰, respectively, and this is in good agreement with the amplitude ($0.8 \pm 0.04$‰) and the mean value ($41.4 \pm 0.04$‰) observed at Hohenpeissenberg.

The $\delta^{18}O$ values of the Mt. Brocken $CO_2$ sampled on 2nd and 28th March 2012 fall within the range observed in Göttingen (40.8‰, 40.1‰ and 40.7‰) (see Fig. 1c, Table 2).

Table 1
Concentration and isotope data of $CO_2$ sampled at Göttingen. The $\Delta^{17}O$ value was determined by a $CO_2$-$CeO_2$ exchange method (Hofmann and Pack, 2010) and the $\Delta^{17}O$ standard error was determined from repeated measurements of the equilibrated $CeO_2$ ($n = 3$–6).

| Sampling date | $CO_2$ [ppm] | $\delta^{13}C_{VPDB}$ [‰] | $\delta^{18}O_{VSMOW}$ [‰] | $\Delta^{17}O$[‰] ($\lambda_{RL} = 0.5229$) | SE $\Delta^{17}O$ [‰] |
|---|---|---|---|---|---|
| 2010/6/7 | 386 | −8.53 | 42.26 | 0.035 | 0.028 |
| 2010/6/30 | 398 | −8.14 | 42.51 | 0.048 | 0.021 |
| 2010/8/18 | 384 | −8.48 | 41.34 | 0.030 | 0.011 |
| 2010/8/20 | 378 | −7.92 | 41.92 | −0.036 | 0.036 |
| 2010/9/1 | 375 | −8.09 | 41.17 | −0.027 | 0.022 |
| 2010/9/21 | 383 | −8.17 | 41.56 | −0.061 | 0.022 |
| 2010/10/12 | 402 | −8.62 | 41.76 | −0.028 | 0.030 |
| 2010/10/20 | 398 | −8.31 | 40.89 | −0.123 | 0.034 |
| 2010/11/5 | 416 | −9.17 | 41.17 | −0.030 | 0.020 |
| 2010/11/19 | 435 | −9.09 | 39.98 | −0.016 | 0.031 |
| 2010/12/17 | 418 | −8.79 | 40.84 | −0.013 | 0.034 |
| 2011/1/10 | 414 | −9.30 | 40.35 | −0.083 | 0.029 |
| 2011/1/28 | 418 | −8.94 | 40.89 | −0.092 | 0.032 |
| 2011/2/4 | 419 | −9.16 | 41.12 | −0.043 | 0.044 |
| 2011/2/28 | 475 | −8.97 | 41.33 | 0.052 | 0.010 |
| 2011/3/18 | 472 | −9.02 | 40.99 | 0.019 | 0.009 |
| 2011/4/1 | 437 | −8.98 | 41.69 | −0.047 | 0.027 |
| 2011/4/29 | 458 | −9.02 | 42.48 | 0.065 | 0.017 |
| 2011/5/6 | 459 | −8.30 | 43.29 | 0.001 | 0.037 |
| 2011/5/13 | 398 | −8.53 | 42.70 | −0.006 | 0.048 |
| 2011/6/9 | 399 | −8.37 | 42.60 | 0.057 | 0.044 |
| 2011/6/24 | 393 | −8.28 | 42.96 | 0.017 | 0.062 |
| 2011/7/8 | 389 | −8.42 | 42.82 | −0.033 | 0.046 |
| 2011/7/25 | 386 | −7.95 | 41.92 | −0.067 | 0.023 |
| 2011/8/5 | 406 | −8.90 | 42.19 | −0.093 | 0.027 |
| 2011/9/15 | 385 | −7.99 | 41.99 | −0.124 | 0.034 |
| 2011/10/28 | 415 | −9.58 | 40.16 | −0.147 | 0.018 |
| 2011/11/11 | 422 | −9.22 | 40.59 | −0.128 | 0.021 |
| 2011/12/9 | 420 | −8.79 | 40.96 | −0.139 | 0.024 |
| 2011/12/22 | 433 | −8.77 | 41.30 | −0.109 | 0.022 |
| 2012/1/6 | 429 | −9.29 | 41.23 | −0.110 | 0.018 |
| 2012/1/27 | 432 | −9.23 | 41.50 | −0.168 | 0.026 |
| | - | −10.35 | 40.36 | −0.154 | 0.026 |
| 2012/2/7 | 427 | −10.29 | 40.43 | −0.202 | 0.025 |
| 2012/2/17 | 435 | −9.64 | 41.35 | −0.206 | 0.032 |
| 2012/3/1 | 433 | −9.54 | 41.49 | −0.135 | 0.032 |
| 2012/3/15 | 419 | −8.84 | 41.89 | −0.113 | 0.030 |
| 2012/3/30 | 415 | −8.99 | 41.97 | −0.035 | 0.031 |
| 2012/4/13 | 396 | −9.36 | 41.31 | −0.105 | 0.008 |
| | | | | −0.037 | 0.013 |
| | | | | −0.071 | 0.010 |
| 2012/4/26 | – | −10.00 | 41.03 | −0.094 | 0.007 |
| 2012/5/9 | 422 | −9.20 | 42.20 | −0.156 | 0.020 |
| 2012/5/23 | 445 | −10.01 | 42.91 | −0.175 | 0.004 |
| 2012/6/6 | 423 | −9.07 | 43.24 | −0.092 | 0.022 |
| 2012/6/20 | 451 | −10.08 | 41.97 | −0.111 | 0.024 |
| 2012/7/4 | 457 | −10.99 | 42.47 | −0.091 | 0.053 |
| 2012/7/18 | 417 | −9.37 | 41.68 | −0.100 | 0.037 |
| 2012/8/1 | 393 | −8.31 | 43.04 | −0.130 | 0.031 |
| 2012/8/15 | 398 | −7.82 | 42.15 | −0.063 | 0.028 |

### 3.4. $\Delta^{17}O(CO_2)$ time series data

The $\Delta^{17}O$ values observed in Göttingen vary between −0.21 and +0.07‰ and show a large drop in $\Delta^{17}O$ between May and October of 2011, which persists through the end of our record (see Fig. 1d). As a result, the annual mean value for our first year ($\Delta^{17}O = -0.02 \pm 0.05$‰ (SD)) differs strongly from the second year ($\Delta^{17}O = -0.12 \pm 0.04$‰ (SD)). Multiple possible causes for this drop were investigated, and included both experimental and physical origins. These are discussed in Sections 5 and 6 alongside with other published observations of the global $\Delta^{17}O$ abundance. However, we note that despite our efforts, the decrease in $\Delta^{17}O$ in our records remain unexplained at this moment.

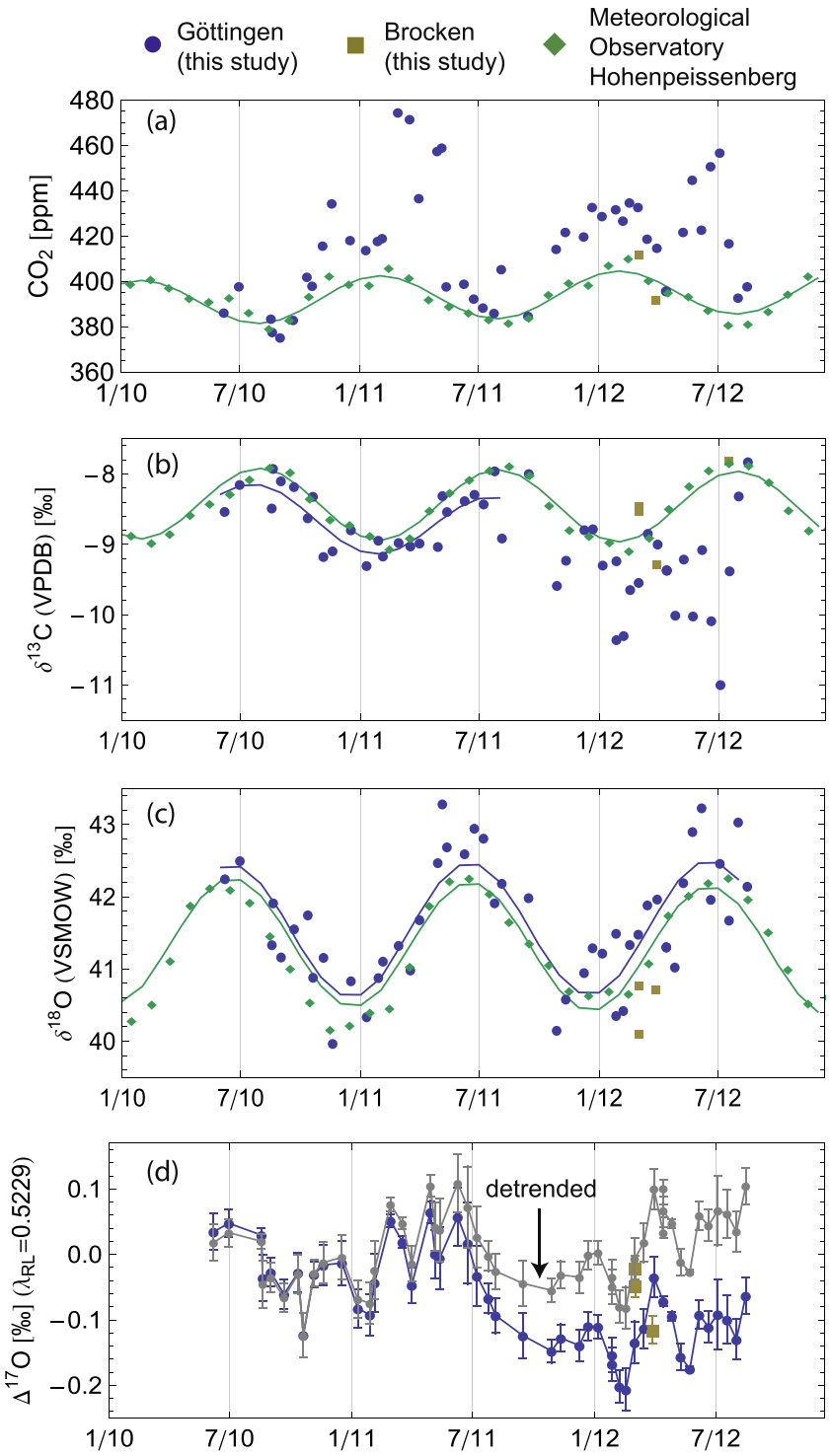


Fig. 1. Time series of $CO_2$ concentration, $\delta^{13}C$ and $\delta^{18}O$ values. (a) The $CO_2$ concentration observed in Göttingen is up to 75 ppm higher than the concentration observed at the Meteorological Observatory Hohenpeissenberg (986 m.a.s.l.) due to local $CO_2$ sources from soil respiration and anthropogenic emissions. The contribution from local $CO_2$ sources tends to be highest during wintertime. The measurement uncertainty for the $CO_2$ concentration data analyzed in this study is about 5 ppm. (b) In the first year, the $\delta^{13}C$ values show a pronounced seasonal cycle, which is in good agreement with the seasonal cycle observed at the Meteorological Observatory Hohenpeissenberg. In the second year, the $\delta^{13}C$ values show a large scatter towards lower values. The measurement uncertainty for $\delta^{13}C$ of $CO_2$ extracted from air is about 0.1‰. (c) The $\delta^{18}O$ values observed in Göttingen show a pronounced seasonal cycle that is in good agreement with the seasonal cycle observed at the Meteorological Observatory Hohenpeissenberg. This seasonality is controlled by high assimilation fluxes during summer and high respiratory fluxes during winter. The measurement uncertainty for $\delta^{18}O$ of $CO_2$ extracted from air is about 0.2‰. (d) The $\Delta^{17}O(CO_2)$ values observed in Göttingen show a seasonal pattern with highest values in June/July. This seasonal cycle is superimposed by a large drop in $\Delta^{17}O$ between May and October of 2011. The possible reasons for this drop are discussed in Section 6.2. In order to focus on the seasonality in $\Delta^{17}O(CO_2)$, we detrended the time series using the curve fitting procedure from Thoning et al. (1989).

Table 2
Concentration and isotope data of $CO_2$ sampled at the Brocken Mountain. The $\Delta^{17}O$ value was determined by a $CO_2$-$CeO_2$ exchange method (Hofmann and Pack, 2010) and the $\Delta^{17}O$ standard error was determined from repeated measurements of the equilibrated $CeO_2$ ($n = 3$–6).

| Sampling date | $CO_2$ [ppm] | $\delta^{13}C_{VPDB}$ [‰] | $\delta^{18}O_{VSMOW}$ [‰] | $\Delta^{17}O$ [‰] ($\lambda_{RL} = 0.5229$) | SE $\Delta^{17}O$ [‰] |
|---|---|---|---|---|---|
| 2012/03/02 | 412 | −8.44 | 40.78 | −0.047 | 0.018 |
| | 412 | −8.52 | 40.11 | −0.020 | 0.018 |
| 2012/03/28 | 392 | −9.27 | 40.73 | −0.115 | 0.021 |

On top of this large drop, we measure a significant seasonal cycle with maximum $\Delta^{17}O$ values in June/July and an amplitude (peak-to-trough) of $0.10 \pm 0.02$‰ (SD) in 2010, $0.15 \pm 0.02$‰ (SD) in 2011 and $0.13 \pm 0.02$‰ (SD) in 2012 yielding an average of $0.13 \pm 0.02$‰ (SD) (see Fig. 1d). The amplitude and the 1-sigma uncertainty are derived from a full time series curve fit using the CCGCRV procedure of NOAA Earth System Research Laboratory (Thoning et al., 1989). In order to investigate this interannual variability further, we detrended the $\Delta^{17}O$ time series using the curve fitting procedure of Thoning et al. (1989). The amplitude (peak-to-trough) of the detrended seasonal cycle is $0.11 \pm 0.02$‰ (SD) in 2010, $0.14 \pm 0.02$‰ (SD) in 2011 and $0.12 \pm 0.02$‰ (SD) in 2012 with an average of $0.13 \pm 0.02$‰ (SD). For both the detrended and non-detrended time series, the amplitude is much larger than our reported measurement precision on a single observation (0.025‰), and the uncertainty on the amplitude confirms that with multiple measurements per season ($N_{winter} = 19$, $N_{summer} = 31$), this signal is resolved very well. This temporal variation is to our knowledge one of the first characterizations of seasonal $\Delta^{17}O$ variability (see also Tables 1 and 2) and our further analysis focuses on the explanation of this seasonal behavior using a global box model of $\Delta^{17}O$, as well as a Göttingen-specific output from a 3-D atmospheric transport model for $\Delta^{17}O$.

## 4. MODEL DESCRIPTION

### 4.1. Global mass balance model

Various $CO_2$ sources and sinks characterize the triple oxygen isotope signature of tropospheric $CO_2$. We consider the following gross fluxes $F$ that affect the tropospheric $CO_2$ reservoir:

$$dM/dt = F_A(t) + F_{resp}(t) + F_{OA}(t) + F_{AO}(t) + F_{SA}(t) + F_{AS}(t) + F_{SIA}(t) + F_{ASI}(t) + F_{ff} + F_{fire} \quad (4\text{-}1)$$

with

$dM/dt$ = rate of increase of tropospheric $CO_2$ reservoir (in PgC/yr),
$F_A$ = terrestrial assimilation flux (in PgC/yr),
$F_{resp}$ = $CO_2$ emitted from terrestrial respiration (in PgC/yr),
$F_{OA}$ = $CO_2$ emitted from the oceans (in PgC/yr),
$F_{AO}$ = $CO_2$ taken up by oceans (in PgC/yr),
$F_{SA}$ = stratospheric $CO_2$ entering the troposphere (in PgC/yr),
$F_{AS}$ = tropospheric $CO_2$ entering the stratosphere (in PgC/yr),
$F_{SIA}$ = soil invasion flux to troposphere (in PgC/yr),
$F_{ASI}$ = soil invasion flux from troposphere (in PgC/yr),
$F_{ff}$ = $CO_2$ emitted from fossil fuel burning (in PgC/yr), and
$F_{fire}$ = $CO_2$ emitted from biomass burning (in PgC/yr).

We use an initial size of 830 PgC ($=M_0$) for the tropospheric $CO_2$ reservoir, i.e. a mixing ratio of 390 ppm, and an increase rate of 4 PgC/yr ($=dM/dt$), i.e. 1.9 ppm/yr (Canadell et al., 2007; Le Quéré et al., 2009). Note that the size of the $CO_2$ fluxes (except $F_{ff}$ and $F_{fire}$) increases as the $CO_2$ concentration$_{fire}$) in the atmosphere increases. The initial magnitudes of the carbon sources and sinks are listed in Table 3 and will be discussed in detail below.

In order to model the global $\delta^{18}O$ composition of tropospheric $CO_2$ ($=\delta_a$), we consider the following global mass balance equation according to previous studies (Ciais et al., 1997; Cuntz et al., 2003a,b; Welp et al., 2011):

$$\frac{d\delta_a}{dt} = \frac{1}{M_0 + (dM/dt)t} \times [F_A(t)\, D_A + F_{resp}(t)\, (\delta_{resp} - \delta_a) + F_{OA}(t)\, (\delta_O - \delta_a) + F_{SA}(t)\, (\delta_{strat} - \delta_a) + F_{SIA}(t)(\delta_{SI} - \delta_a) + F_{ff}(\delta_{ff} - \delta_a) + F_{fire}(\delta_{fire} - \delta_a)] \quad (4\text{-}2)$$

with

$M_0$ = initial size of tropospheric $CO_2$ reservoir (in PgC),
$D_A$ = $\delta^{18}O$ isotope discrimination due to assimilation (in ‰), i.e. kinetic fractionation during diffusion into and out of leaf stomata and $CO_2$-water equilibration in the stomata,
$\delta_{resp}$ = $\delta^{18}O$ value of $CO_2$ emitted from terrestrial respiration (in ‰),
$\delta_O$ = $\delta^{18}O$ value of $CO_2$ emitted from the ocean (in ‰),
$\delta_{strat}$ = $\delta^{18}O$ value of $CO_2$ from the lower stratosphere (in ‰),
$\delta_{SI}$ = $\delta^{18}O$ value of $CO_2$ in equilibrium with soil water (in ‰),
$\delta_{ff}$ = $\delta^{18}O$ value of $CO_2$ from fossil fuel burning (in ‰), and
$\delta_{fire}$ = $\delta^{18}O$ value of $CO_2$ from biomass burning (in ‰).

For the mass balance equations we abbreviate $\delta^{18}O$ values with $\delta$. The isotopic signatures are listed in Table 4 and will also be discussed in detail below. In Eq. (4-2), we can omit the carbon sinks $F_{AO}$, $F_{AS}$ and $F_{ASI}$ because the $\delta$-values of the transported $CO_2$ are identical to $\delta_a$.

In accordance with the global budget equation for the $\delta^{18}O$ composition of the troposphere (Eq. (4-2)), we calculate the $\Delta^{17}O$ signature of tropospheric $CO_2$ ($=\Delta^{17}_a$):

Table 3
Mass balance variables: carbon fluxes and related parameters.

| Parameter | Description | Estimate | Units | References |
|---|---|---|---|---|
| $M_0$ | $CO_2$ inventory troposphere | 830 | PgC | Canadell et al. (2007), Le Quéré et al. (2009) |
| $dM/dt$ | Rate of increase of tropospheric $CO_2$ reservoir | 4 | PgC/yr | Canadell et al. (2007), Le Quéré et al. (2009) |
| $GPP$ | Gross primary production | 120 | PgC/yr | Beer et al. (2010) |
| $F_A = 0.88 \times GPP$ | Terrestrial assimilation rate | 106 | PgC/yr | Ciais et al. (1997) |
| $F_{LA} = F_A \times C_{cs}/(C_a - C_{cs})$ | From leaves | 246 | PgC/yr | Farquhar et al. (1993) |
| $F_{LAequ} = \Theta \times F_{LA}$ | $CO_2$ fraction from leaves that is in equilibrium with leaf water | 197 | PgC/yr | Gillon and Yakir (2000, 2001) |
| $F_{LAnonequ} = (1 - \Theta) \times F_{LA}$ | $CO_2$ fraction from leaves that is not in equilibrium with leaf water | 49 | PgC/yr | Gillon and Yakir (2000, 2001) |
| $F_{AL} = -F_A \times C_a/(C_a\text{-}C_{cs})$ | To leaves | −352 | PgC/yr | Farquhar et al. (1993) |
| $F_{resp} = F_A - 3$ PgC/yr | From terrestrial respiration | 103 | PgC/yr | Canadell et al. (2007), Le Quéré et al. (2009) |
| $F_{SA}$ | From stratosphere | 100 | PgC/yr | Appenzeller et al. (1996) |
| $F_{AS}$ | To stratosphere | −100 | PgC/yr | Appenzeller et al. (1996) |
| $F_{OA}$ | From ocean | 90 | PgC/yr | Heimann and Maier-Reimer (1996) |
| $F_{AO}$ | To ocean | −92 | PgC/yr | Canadell et al. (2007), Le Quéré et al. (2009) |
| $F_{SIA}$ | Soil invasion ($CO_2$ source) | 30 | PgC/yr | Stern et al. (2001) |
| $F_{ASI}$ | Soil invasion ($CO_2$ sink) | −30 | PgC/yr | Stern et al. (2001) |
| $F_{ff}$ | Fossil fuels | 8 | PgC/yr | Boden et al. (2011) |
| $F_{fire}$ | Fire emissions | 1 | PgC/yr | van der Werf et al. (2004), Canadell et al. (2007), Le Quéré et al. (2009) |
| $\Theta = f_{C3}\ \Theta_{C3} + f_{C4}\ \Theta_{C4}$ | Degree of $CO_2$-water equilibration in plant leaves | 0.80 | – | Gillon and Yakir (2000, 2001) |
| $\Theta_{C3}$ | Degree of $CO_2$-water equilibration in $C_3$ plants | 0.93 | – | Gillon and Yakir (2000, 2001) |
| $\Theta_{C4}$ | Degree of $CO_2$-water equilibration in $C_4$ plants | 0.38 | – | Gillon and Yakir (2000, 2001) |
| $f_{C3}$ | Fraction of $C_3$ plants | 0.77 | – | Still et al. (2003) |
| $f_{C4} = (1 - f_{C3})$ | Fraction of $C_4$ plants | 0.23 | – | Still et al. (2003) |
| $C_{cs}/C_a$ | $CO_2$ concentration gradient between chloroplasts and atmosphere | 0.70 | – | Ciais et al. (1997), Cuntz et al. (2003a,b) |

$$\frac{d\Delta_a^{17}}{dt} = \frac{1}{M_0 + (dM/dt)\,t} \times [F_A(t)\,D_A^{17} + F_{resp}(t)\,(\Delta_{resp}^{17} - \Delta_a^{17}) + F_{OA}(t)\,(\Delta_O^{17} - \Delta_a^{17}) + F_{SA}(t)\,(\Delta_{strat}^{17} - \Delta_a^{17}) + F_{SIA}(t)\,(\Delta_{SI}^{17} - \Delta_a^{17}) + F_{ff}\,(\Delta_{ff}^{17} - \Delta_a^{17}) + F_{fire}\,(\Delta_{fire}^{17} - \Delta_a^{17})] \quad (4\text{-}3)$$

with

$D_A^{17} = \Delta^{17}$O isotope discrimination due to assimilation (in ‰), i.e. kinetic fractionation during diffusion into and out of leaf stomata and $CO_2$-water equilibration in the stomata,
$\Delta_{resp}^{17} = \Delta^{17}$O value of $CO_2$ emitted from terrestrial respiration (in ‰),
$\Delta_O^{17} = \Delta^{17}$O value of $CO_2$ in equilibrium with ocean water (in ‰),
$\Delta_{strat}^{17} = \Delta^{17}$O value of $CO_2$ from the lower stratosphere (in ‰),
$\Delta_{SI}^{17} = \Delta^{17}$O value of $CO_2$ in equilibrium with soil water (in ‰),
$\Delta_{ff}^{17} = \Delta^{17}$O value of $CO_2$ from fossil fuel burning (in ‰),
$\Delta_{fire}^{17} = \Delta^{17}$O value of $CO_2$ from biomass burning (in ‰), and
$\lambda_{kinetic}$ = triple oxygen isotope exponent for kinetic fractionation.

For the model description, we abbreviate $\Delta^{17}$O values with $\Delta^{17}$. Both mass balance equations reach a quasi steady-state after a few years, and thus, all model results are given for $t = 50$ yr.

Note that strictly speaking the $\Delta^{17}$O mass balance formulation gives only an approximation for $\Delta_a^{17}$. To be precise, a $\delta^{17}$O mass balance equation would be more appropriate, however, our approximation with $\Delta^{17}$O values changes the final outcome by less than 0.002‰.

#### 4.1.1. Terrestrial assimilation

The terrestrial biosphere fixes about 120 PgC per year (Beer et al., 2010). This rate of carbon fixation by the biosphere is generally termed gross primary production (GPP). Ciais et al. (1997) estimate that about 12% of the annual GPP are consumed by leaf respiration. Furthermore, we assume that the rate of assimilation increases as the $CO_2$ concentration increases:

$$F_A(t) = 0.88\ GPP \left(1 + \frac{dM/dt}{M_0} t\right). \quad (4\text{-}4)$$

The assimilation rate of the terrestrial biosphere is driven by the difference in $CO_2$ concentration in the leaf stomata ($C_{cs}$) and the atmosphere ($C_a$) (Farquhar et al., 1993):

$$F_A = \frac{C_a}{C_a - C_{cs}} F_A - \frac{C_{cs}}{C_a - C_{cs}} F_A = -(F_{LA} + F_{AL}) \quad (4\text{-}5)$$

where $F_{LA}$ denotes the amount of $CO_2$ that is released per year from the stomata to the atmosphere and $F_{AL}$ is the

Table 4
Mass balance variables: isotopic signatures, fractionation factors and related parameters. For the model description, $\delta^{18}O$ values are abbreviated with $\delta$ and $\Delta^{17}O$ values are abbreviated with $\Delta^{17}$.

| Parameter | Description | Estimate | Units | References |
|---|---|---|---|---|
| $\delta_a$ | Modeled $\delta^{18}O$ value of global tropospheric $CO_2$ | | ‰ | |
| $D_A$ | $\delta^{18}O$ isotope discrimination of $CO_2$ due to assimilation | | ‰ | |
| $\delta_L$ | $\delta^{18}O$ value of $CO_2$ in equilibrium with leaf water | 44.7 | ‰ | Ciais et al. (1997) |
| $\delta_{SW}$ | $\delta^{18}O$ value of soil water | −7.5 | ‰ | Ciais et al. (1997) |
| $\delta_{resp}$ | $\delta^{18}O$ value of $CO_2$ emitted from terrestrial respiration | 28.6 | ‰ | Ciais et al. (1997, 2005), Cuntz et al. (2003a,b) |
| $\delta_{ocean}$ | $\delta^{18}O$ value of ocean surface water | 0 | ‰ | |
| $\delta_O$ | $\delta^{18}O$ value of $CO_2$ in equilibrium with ocean water | 42.6 | ‰ | Ciais et al. (1997, 2005), Cuntz et al. (2003a,b) |
| $\delta_{strat}$ | $\delta^{18}O$ value of $CO_2$ from the lower stratosphere | $\delta_a + 0.4‰$ | ‰ | Kawagucci et al. (2008) |
| $\delta_{SI}$ | $\delta^{18}O$ value of $CO_2$ in equilibrium with soil water | 36.0 | ‰ | Wingate et al. (2009) |
| $\delta_{ff}$ | $\delta^{18}O$ value of $CO_2$ from fossil fuel burning | 25 | ‰ | Horváth et al. (2012) |
| $\delta_{fire}$ | $\delta^{18}O$ value of $CO_2$ from biomass burning | 19 | ‰ | Horváth et al. (2012) |
| $\Delta_a^{17}$ | Modeled $\Delta^{17}O$ value of global tropospheric $CO_2$ | | ‰ | |
| $D_A^{17}$ | $\Delta^{17}O$ isotope discrimination due to assimilation | | ‰ | |
| $\Delta_L^{17}$ | $\Delta^{17}O$ value of $CO_2$ in equilibrium with leaf water | −0.059 | ‰ | |
| $\Delta_{SW}^{17}$ | $\Delta^{17}O$ value of soil water | −0.005 | ‰ | |
| $\Delta_{resp}^{17}$ | $\Delta^{17}O$ value of $CO_2$ emitted from terrestrial respiration | 0.095 | ‰ | |
| $\Delta_{ocean}^{17}$ | $\Delta^{17}O$ value of ocean surface water | −0.005 | ‰ | Luz and Barkan (2010) |
| $\Delta_O^{17}$ | $\Delta^{17}O$ value of $CO_2$ in equilibrium with ocean water | −0.005 | ‰ | |
| $\Delta_{strat}^{17}$ | $\Delta^{17}O$ value of $CO_2$ from the lower stratosphere | $\Delta_a^{17} + 0.445‰$ | ‰ | Boering et al. (2004), Kawagucci et al. (2008) |
| $\Delta_{SI}^{17}$ | $\Delta^{17}O$ value of $CO_2$ in equilibrium with soil water | −0.005 | ‰ | |
| $\Delta_{ff}^{17}$ | $\Delta^{17}O$ value of $CO_2$ from fossil fuel burning | −0.386 | ‰ | Horváth et al. (2012) |
| $\Delta_{fire}^{17}$ | $\Delta^{17}O$ value of $CO_2$ from biomass burning | −0.230 | ‰ | Horváth et al. (2012) |
| $\alpha_{CO_2\text{-water}}$ | Temperature dependent equilibrium fractionation factor for $^{18}O/^{16}O$ isotope exchange between $CO_2$ and water | $(17.604/T - 0.01793) + 1$ | – | Brenninkmeijer et al. (1983) |
| $\theta_{CO_2\text{-water}}$ | Triple oxygen isotope equilibrium fractionation factor | 0.5229 | – | Barkan and Luz (2012) |
| $\alpha_{transpiration}$ | Leaf water enrichment in $^{18}O$ due to evapotranspiration | 0.9917 | – | West et al. (2008) |
| $\lambda_{transpiration}$ | triple oxygen isotope fractionation factor for transpiration in plant leaves | $0.522 - 0.008 \times h$ | – | Landais et al. (2006) |
| $h$ | Mean humidity above leaf stomata | 0.8 | – | Ciais et al. (1997) |
| $\alpha_L$ | Kinetic fractionation factor ($^{18}O/^{16}O$) for diffusion into and out of stomata | 0.9926 | – | Farquhar et al. (1993) |
| $\alpha_S$ | Kinetic fractionation factor ($^{18}O/^{16}O$) for diffusion out of soils | 0.9928 | – | Miller et al. (1999) |
| $\lambda_{kinetic}$ | Triple oxygen isotope factor for kinetic fractionation | 0.509 | – | Young et al. (2002) |
| $\lambda_{RL}$ | Slope of reference line ($CO_2$-water equilibration line) | 0.5229 | – | Barkan and Luz (2012) |
| $\lambda_{GMWL}$ | Slope of the global meteoric water line | 0.528 | – | Luz and Barkan (2010) |
| $\gamma_{GMWL}$ | Intercept of the global meteoric water line | 0.033 | ‰ | Luz and Barkan (2010) |
| $T_{soil}$ | Global mean soil temperature | 285 | K | Ciais et al. (1997) |
| $T_{leaf}$ | Global mean leaf temperature | 285 | K | Ciais et al. (1997) |
| $T_{ocean}$ | Global mean sea surface temperature | 291 | K | Ciais et al. (1997) |

amount of $CO_2$ diffusing into terrestrial leaf stomata. The $C_{cs}/C_a$ ratio varies between $C_3$ and $C_4$ plants because the latter fix carbon dioxide more effectively due to a different photosynthetic pathway (Pearcy and Ehleringer, 1984). For the mass balance calculation we assume an overall $C_{cs}/C_a$ ratio of 0.70 (Ciais et al., 1997; Cuntz et al., 2003a,b), which takes into account that about 77% of the global GPP can be traced back to $C_3$ plants ($f_{C3}$) and the remaining to $C_4$ plants ($f_{C4}$) (Lloyd and Farquhar, 1994; Still et al., 2003).

The $CO_2$ diffusing into the leaf stomata rapidly exchanges its oxygen isotopes with the leaf water. For $C_3$ plants, about 93% of the $CO_2$ diffusing out of the stomata is in isotopic equilibrium with leaf water ($\Theta_{C3} = 0.93$) and for $C_4$ plants about 38% of the $CO_2$ is in isotopic equilibrium ($\Theta_{C4} = 0.38$) (Gillon and Yakir, 2000, 2001). Thus, we can estimate the fraction of $CO_2$ that is in equilibrium with leaf water ($F_{LAequ}$) and the fraction of $CO_2$ that is not affected by exchange with leaf water ($F_{LAnonequ}$):

$$F_{LAequ} = (f_{C3} \times \Theta_{C3} + f_{C4} \times \Theta_{C4}) \times F_{LA} \quad (4\text{-}6)$$

and

$$F_{LAnonequ} = (f_{C3} \times (1 - \Theta_{C3}) + f_{C4} \times (1 - \Theta_{C4})) \times F_{LA}. \quad (4\text{-}7)$$

The $^{18}O/^{16}O$ ratio of $CO_2$ in equilibrium with leaf water ($\delta_L$) depends on (i) the isotopic composition of the soil and stem water ($\delta_{SW} = -7.5‰$, Ciais et al., 1997), (ii) the degree of kinetic fractionation due to evapotranspiration in the leaves ($\alpha_{transpiration} = 0.9917$, West et al., 2008) and (iii) the equilibration temperature ($T_{leaf} = 285$ K, Ciais et al., 1997):

$$\delta_L = (\delta_{SW} + 1)\frac{\alpha_{CO_2-water}(T_{leaf})}{\alpha_{transpiration}} \quad (4\text{-}8)$$

where $\alpha_{CO_2\text{-water}}$ is the temperature dependent $^{18}O/^{16}O$ fractionation factor for $CO_2$-water exchange according to Brenninkmeijer et al. (1983).

The effect of carbon assimilation during photosynthesis on the $^{18}O/^{16}O$ ratio in atmospheric $CO_2$ can then be expressed as:

$$F_A \times D_A = (\alpha_L - 1) \times (F_{AL} + F_{LAnonequ}) + ((\delta_L + 1) \times \alpha_L - 1 - \delta_a) \times F_{LAequ} \quad (4\text{-}9)$$

where $\alpha_L = 0.9926$ describes the kinetic fractionation factor for diffusion into and out of the stomata (Farquhar et al., 1993) and the product $F_A \times D_A$ describes the assimilation isoflux. The term isoflux is commonly used to refer to the multiplication of the carbon flux size and the isotopic effect relative to the isotopic composition of tropospheric $CO_2$.

Similar to $^{18}O/^{16}O$, the triple oxygen isotope composition of $CO_2$ emitted from plants depends on the oxygen isotope signature of soil water. We assume that the triple oxygen isotope composition of soil water ($\Delta^{17}_{SW}$) at the depth where plant roots take up water is not affected by evaporation and that it falls on the global meteoric water line (GMWL) with a slope $\lambda_{GMWL} = 0.528$ and an intercept $\gamma_{GMWL} = 0.033‰$ (Luz and Barkan, 2010):

$$\Delta^{17}_{SW} = (\lambda_{GMWL} - \lambda_{RL}) \times \ln(\delta_{SW} + 1) + \gamma_{GMWL}. \quad (4\text{-}10)$$

Given this relationship, soil water with $\delta_{SW} = -7.5‰$ has a $\Delta^{17}_{SW}$ value of $-0.005‰$.

The triple oxygen isotope composition of $CO_2$ in equilibrium with leaf water ($\Delta^{17}_L$) depends on (i) the isotopic composition of the soil water, (ii) the degree of evapotranspiration and (iii) the oxygen isotope exchange between $CO_2$ and water in the stomata (see Fig. 2):

$$\Delta^{17}_L = \Delta^{17}_{SW} + (\lambda_{RL} - \lambda_{transpiration}) \times \ln(\alpha_{transpiration}) + (\lambda_{RL} - \theta_{CO_2\text{-water}}) \times \ln(\alpha_{CO_2\text{-water}}(T_{leaf})) \quad (4\text{-}11)$$

where $\theta_{CO_2\text{-water}}$ is the exponent for triple oxygen isotope exchange between $CO_2$ and water and $\lambda_{transpiration}$ the exponent for transpiration in plant leaves. Barkan and Luz (2012) determined an exponent $\theta_{CO_2\text{-water}}$ of 0.5229 ± 0.0001 for 25 °C. For the exponent $\lambda_{transpiration}$, Landais et al. (2006) showed that it depends on the mean humidity $h$ above the leaf stomata: $\lambda_{transpiration} = 0.522–0.008 \times h$. Note that the slope of the reference line $\lambda_{RL}$ is equal to the exponent $\theta_{CO_2\text{-water}}$ and for this particular case the last term becomes zero.

The $^{17}O/^{16}O$ isoflux for photosynthetic activity of terrestrial plants (in ‰PgC/yr) can be calculated according to the $^{18}O/^{16}O$ isoflux (see Eq. (4-9)):

$$F_A \times \Delta^{17}_A = (\ln(\alpha_L) \times (\lambda_{kinetic} - \lambda_{RL})) \times (F_{AL} + F_{LAnonequ}) + (\Delta^{17}_L + (\lambda_{kinetic} - \lambda_{RL}) \times \ln(\alpha_L) - \Delta^{17}_a) \times F_{LAequ}. \quad (4\text{-}12)$$

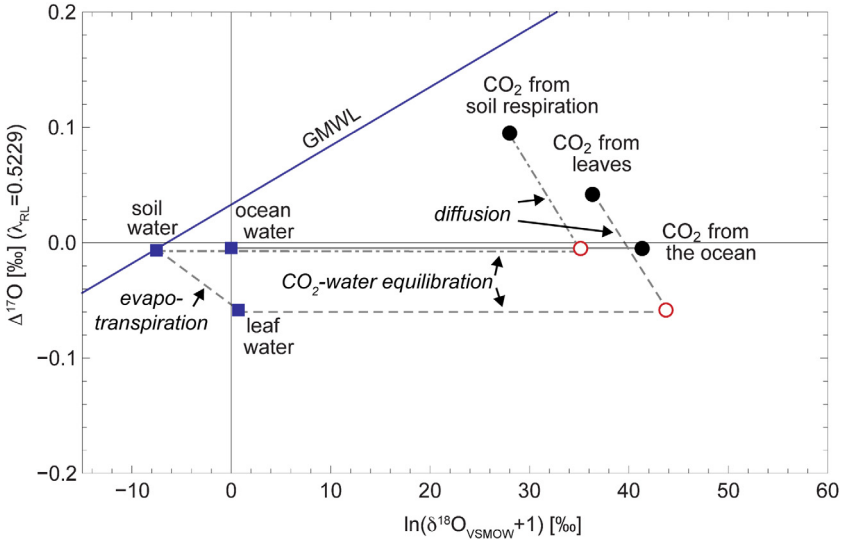


Fig. 2. Triple oxygen isotope signature of the main mass-dependently fractionated $CO_2$ sources to the troposphere. The squares illustrate the triple oxygen isotope composition of the main water reservoirs (ocean, soil and leaf water); the closed circles illustrate the isotopic composition of the $CO_2$ emitted from ocean, soils and terrestrial plants. We assume that equilibration between carbon dioxide and the three water reservoirs takes place with $\theta_{CO_2\text{-water}} = 0.5229 \pm 0.0001$ (Barkan and Luz, 2012), i.e. parallel to the slope of our reference line $\lambda_{RL}$. Carbon dioxide released from the oceans is in isotopic equilibrium with ocean surface water. Carbon dioxide released from plant leaves is in isotopic equilibrium with leaf water which deviates from the global meteoric water line (GMWL, Luz and Barkan, 2010) due to kinetic fractionation during evapotranspiration with $\lambda_{transpiration} = 0.516$ for a relative humidity of 0.8 (Landais et al., 2006). Carbon dioxide produced in soils equilibrates with soil water (open circle), but subsequently the $CO_2$ is kinetically fractionated due to diffusion out of the soil column (Miller et al., 1999) with $\lambda_{kinetic} = 0.509$. Carbon dioxide emitted from leaves is also affected by kinetic fractionation during diffusion.

Eq. (4-12) illustrates that all the $CO_2$ diffusing into and out of the stomata is kinetically fractionated, but only a part of the $CO_2$ equilibrates with leaf water before retro-diffusing into the atmosphere.

*4.1.2. Respiration and soil invasion*

Most of the carbon assimilated by terrestrial photosynthesis is eventually released back to the atmosphere as $CO_2$ due to soil respiration. The net carbon sink due to terrestrial carbon assimilation is about 3 PgC/yr (Canadell et al., 2007; Le Quéré et al., 2009):

$$F_{resp}(t) = F_A(t) - 3\,\mathrm{PgC}/yr. \quad (4\text{-}13)$$

Based on our assumption on GPP and the relationship given above, the flux from terrestrial respiration is 102.6 PgC/yr.

Carbon dioxide produced by soil respiration rapidly equilibrates with soil water at a global mean temperature of 12 °C (Ciais et al., 1997). Subsequently, it is kinetically fractionated during the diffusion process out of the soil column with $\alpha_S = 0.9928$ (Miller et al., 1999):

$$\delta_{resp} = (\delta_{SW} + 1)\alpha_{CO_2-water}(T_{soil})\alpha_S - 1. \quad (4\text{-}14)$$

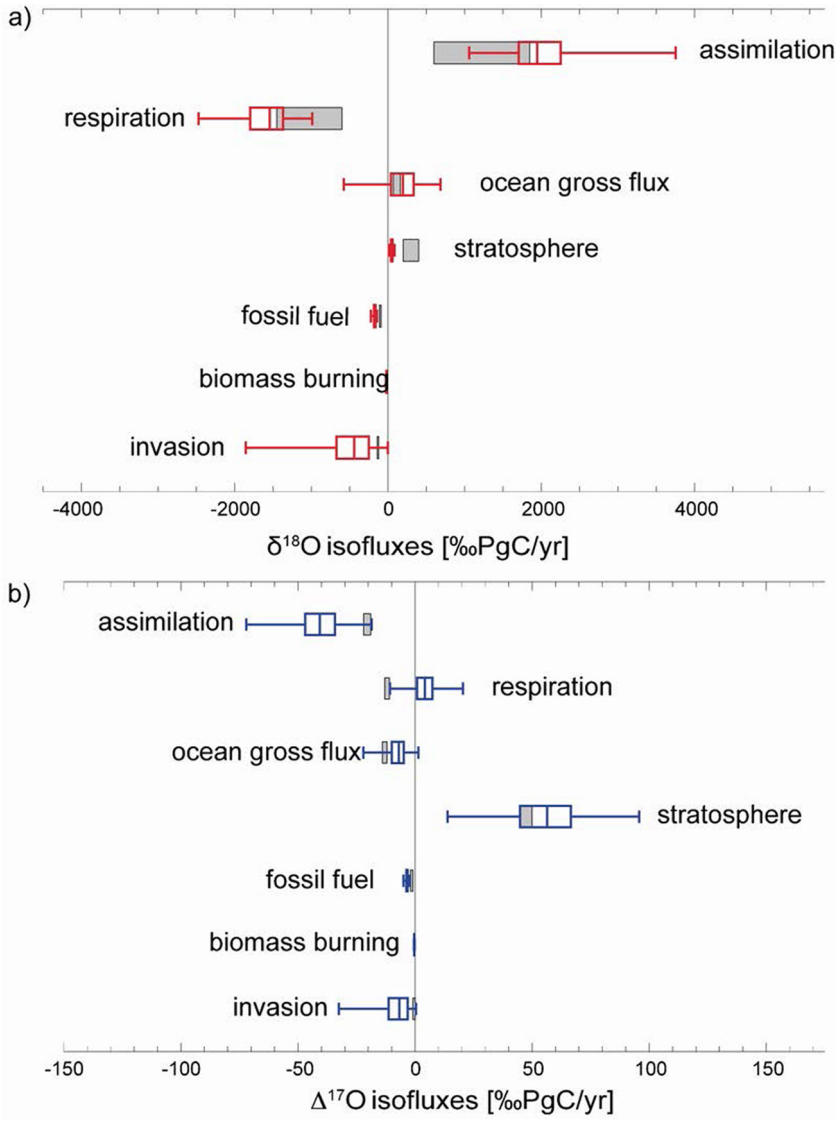


Fig. 3. Box plots showing the main isofluxes controlling the triple oxygen isotope composition of tropospheric $CO_2$. The boxes indicate the median, 25th and 75th percentiles of the Monte Carlo simulation. The whisker caps indicate 5th and 95th percentiles. (a) $\delta^{18}O$ isofluxes: The $\delta^{18}O$ composition of tropospheric $CO_2$ is mainly controlled by two opponents: assimilation and respiration. The $\delta^{18}O$ model assumptions in this study are in good agreement with previous $\delta^{18}O$ isofluxes from Ciais et al. (2005) (gray rectangles). The only major modification is the assumption on the soil invasion flux: We implemented a mean of 30 PgC/yr in the Monte Carlo simulation, but extended the possible range up to 450 PgC/yr as suggested by Wingate et al. (2009). (b) $\Delta^{17}O$ isofluxes: The model suggests that the $\Delta^{17}O$ value of tropospheric $CO_2$ is mainly controlled by assimilation, respiration, soil invasion and stratospheric influx. However, in contrast to the model from Hoag et al. (2005) (gray rectangles), our modeling results suggest that both respiratory $CO_2$ and stratospheric influx have a positive effect on $\Delta^{17}O$ of tropospheric $CO_2$ and the soil invasion flux might also significantly affect the triple oxygen isotope composition of tropospheric $CO_2$.

Analogous to $\delta_{resp}$, we estimate the triple oxygen isotope composition of soil respired $CO_2$:

$$\Delta^{17}_{resp} = \Delta^{17}_{SW} - (\lambda_{RL} - \theta_{CO_2\text{-water}}) \times \ln(\alpha_{CO_2\text{-water}}(T_{soil})) - (\lambda_{RL} - \lambda_{kinetic}) \times \ln(\alpha_S). \quad (4\text{-}15)$$

$CO_2$ diffusing into the uppermost soil column equilibrates with soil water and diffuses back to the atmosphere. This process is known as the soil invasion flux (Tans, 1998; Miller et al., 1999). We take a soil invasion flux $F_{SI}$ of 30 PgC per year (Stern et al., 2001). Recently, Wingate et al. (2009) suggested that the soil invasion flux might account for up to 450 PgC/yr and we considered this estimate as an upper limited for the soil invasion flux in the Monte Carlo simulation (see below section on the Monte Carlo simulation).

The isotopic composition of the soil invasion flux depends on the global mean soil water isotope composition and on the equilibration temperature in the soils:

$$\delta_{SI} = (\delta_{SW} + 1) \times \alpha_{CO_2-water}(T_{soil}) - 1. \quad (4\text{-}16)$$

Analog to $\delta_{SI}$, we estimate the triple oxygen isotope signature of the soil invasion flux:

$$\Delta^{17}_{SI} = \Delta^{17}_{SW} - (\lambda_{RL} - \theta_{CO_2\text{-water}}) \times \ln(\alpha_{CO_2-water}(T_{soil})). \quad (4\text{-}17)$$

#### 4.1.3. Ocean gross fluxes

We assume that the gross $CO_2$ flux from the oceans to the troposphere is about 90 PgC/yr (Heimann and Maier-Reimer, 1996):

$$F_{OA}(t) = 90\,\text{PgC}/yr \left(1 + \frac{dM/dt}{M_0} t\right). \quad (4\text{-}18)$$

Global carbon models generally consider a constant net ocean sink of 2 PgC/yr (Canadell et al., 2007; Le Quéré et al., 2009). However, we omit the carbon sink flux for triple oxygen isotope calculations because the oxygen isotope fractionation occurring at the air-sea interface is negligible (e.g. Ciais et al., 2005).

The mean oxygen isotope composition of ocean water is $\delta_{ocean} = 0‰$ and $\Delta^{17}_{ocean} = -0.005‰$ (Luz and Barkan, 2010). The $CO_2$ diffusing into the ocean surface water equilibrates rapidly with the ocean water at a global mean temperature of 18 °C (Ciais et al., 1997). It follows from the above that

$$\delta_O = (\delta_{ocean} + 1) \times \alpha_{CO_2\text{-water}}(T_{ocean}) - 1 \quad (4\text{-}19)$$

and

$$\Delta^{17}_O = \Delta^{17}_{ocean} - (\lambda_{RL} - \theta_{CO_2\text{-water}}) \times \ln(\alpha_{CO_2\text{-water}}(T_{soil})). \quad (4\text{-}20)$$

#### 4.1.4. Stratosphere-troposphere exchange fluxes

The $CO_2$ fluxes from the troposphere into the stratosphere and vice versa are 100 PgC/yr and −100 PgC/yr, respectively (Appenzeller et al., 1996). Because the $CO_2$ flux leaving the troposphere is not fractionated, we only have to consider the $CO_2$ source entering the troposphere:

$$F_{SA}(t) = 100\,\text{PgC/yr} \left(1 + \frac{dM/dt}{M_0} t\right). \quad (4\text{-}21)$$

Carbon dioxide from the stratosphere is enriched in $^{18}O$ due to isotopic exchange with stratospheric ozone (Gamo et al., 1989). Kawagucci et al. (2008) estimate the oxygen isotope fluxes for stratospheric carbon dioxide to the troposphere based on a linear correlation between the $N_2O$ mixing ratio and the $\delta^{18}O$ composition of $CO_2$. For $\delta^{18}O$, the authors give +38‰PgC/yr. Combining their data with an estimate for the $CO_2$ flux size of 100 PgC/yr (Appenzeller et al., 1996), we assume that stratospheric $CO_2$ is enriched relative to tropospheric $CO_2$ by 0.4‰:

$$\delta_{strat} = \delta_a + 0.4‰ \quad (4\text{-}22)$$

Similar to $\delta^{18}O$, the $^{17}O$ enrichment of the stratospheric $CO_2$ flux to the troposphere can be estimated on combined $\Delta^{17}O$ ($CO_2$) and $N_2O$ measurements of stratospheric air masses (Boering et al., 2004; Kawagucci et al., 2008). Boering et al. (2004) determined a net $CO_2$ flux from the stratosphere of 42.9‰PgC/yr and Kawagucci et al. (2008) determined a value of 48 ‰PgC/yr. Recasting these literature data relative to our reference line with $\lambda_{RL} = 0.5229$ in a triple oxygen isotope plot with logarithmic $\delta$-coordinates gives 42‰PgC/yr and 47‰PgC/yr, respectively. We take an average value of 44.5‰PgC/yr and combine it with the stratospheric flux size of 100 PgC/yr (Appenzeller et al., 1996) to estimate the $\Delta^{17}O$ value of stratospheric $CO_2$ entering the troposphere:

$$\Delta^{17}_{strat} = \Delta^{17}_a + 0.445‰. \quad (4\text{-}23)$$

#### 4.1.5. Anthropogenic emissions and biomass burning

Carbon dioxide from anthropogenic emissions and biomass burning are minor carbon fluxes on a global scale compared to the large gross carbon fluxes from the terrestrial biosphere. Anthropogenic $CO_2$ emissions from fossil fuel burning amount to about 9 PgC/yr (Canadell et al., 2007; Le Quéré et al., 2015). Global fire emissions are estimated to contribute about 1 PgC/yr to global $CO_2$ sources (van der Werf et al., 2004; Canadell et al., 2007; Le Quéré et al., 2015).

It may be assumed that $CO_2$ from fossil fuel combustion or biomass burning largely inherits its triple oxygen isotope composition from atmospheric $O_2$. Barkan and Luz (2011) determined the triple oxygen isotope composition of tropospheric $O_2$ with $\delta^{18}O = 23.881‰$ and $\Delta^{17}O = -0.386‰$ (relative to a reference line with $\lambda_{RL} = 0.5229$). Horváth et al. (2012) showed that $CO_2$ from high-temperature combustion, indeed, produces $CO_2$ with a triple oxygen isotope composition that is close to that of ambient air $O_2$ ($\delta^{18}O \approx \sim 22‰$ and $\Delta^{17}O \approx -0.33‰$ relative to $\lambda_{RL} = 0.5229$). However, car exhaust is significantly enriched in $^{18}O$ ($\delta^{18}O = 33‰$), but it also inherits the oxygen isotope anomaly of air $O_2$ ($\Delta^{17}O = -0.34‰$) (Horváth et al., 2012). For this study, we assume that anthropogenic $CO_2$ from fossil fuel burning inherits to a large extent the oxygen isotope composition of ambient air $O_2$ and that $CO_2$ from fossil fuel combustion has $\delta_{ff} = 25‰$ and $\Delta^{17}_{ff} = -0.34‰$. The triple oxygen isotope composition of carbon dioxide from

low temperature combustion, such as wood combustion, is affected by equilibration with water or other oxygen sources, e.g. wood inherent oxygen (Horváth et al., 2012). Thus, we assume that $CO_2$ produced from biomass burning has $\delta_{fire} = 19‰$ and $\Delta^{17}_{fire} = -0.23‰$ (Horváth et al., 2012).

#### 4.1.6. Monte Carlo simulation

We carried out a Monte Carlo simulation in order to obtain an uncertainty estimate of the $\delta^{18}O$ and $\Delta^{17}O$ mass balance output. The input parameters that were considered for the Monte Carlo simulation are listed in Table 5. The parameters were independently varied using a random function that produces values according to a normal distribution. The mean, standard deviation and maximum-minimum values were chosen according to the literature. For all parameters, the range of variation represents the broadest reasonable distribution. The simulation was carried out with 1000 random numbers for each variable. Additionally, we tested the sensitivity of $\Delta^{17}O$ of tropospheric $CO_2$ to the size of terrestrial gross primary productivity.

### 4.2. Simulating the temporal variability of $\Delta^{17}O$ of tropospheric $CO_2$ with a global atmosphere-biosphere model

We additionally use results from the offline Tracer Transport Model TM5 that simulated the 3-dimensional atmospheric variations of $\Delta^{17}O$ in $CO_2$. The TM5 model is a well-tested tool for atmospheric transport studies and has been previously used to simulate a wide range of tracers including $CO_2$ (Peters et al., 2010), $CH_4$ (Meirink et al., 2008), $SF_6$ (Peters, 2004), and CO (Krol et al., 2013). Further information on TM5 can be found in Huijnen et al. (2010). To simulate $\Delta^{17}O$ in $CO_2$ we implemented separate tracers for $^{16}O$, $^{17}O$ and $^{18}O$ in $CO_2$ and subsequently calculated offline $\Delta^{17}O$ values for all grid boxes according to Eq. (4-3). Fractionation processes and pool signatures were implemented to follow the equations in the global box model described above, leaving only the explicit spatiotemporal surface fluxes and initial mixing ratios of $CO_2$ that differ, and are therefore described.

Surface fluxes of $CO_2$ and atmospheric initial conditions were derived from CarbonTracker (Peters et al., 2010 and http://www.carbontracker.eu). The terrestrial biosphere in CarbonTracker is simulated using the SIBCASA biosphere model documented fully in Schaefer et al. (2008) and van der Velde et al. (2014). In addition to *GPP* and *TER* (total ecosystem respiration), SIBCASA calculates explicitly the values of $C_i/C_a$ allowing the calculation of gross atmosphere-leaf fluxes ($F_{AL}$) and leaf-atmosphere fluxes ($F_{AL}$), and uses $C_3/C_4$ dependent equilibration factors (see Eq. (4-7)). Because the magnitude of the soil invasion isoflux is highly uncertain (Wingate et al., 2009), we assume this flux to be a fixed ratio $r_{soil}$ of terrestrial respiration. We performed simulations with $r_{soil}$ of 0.3, 1.0 and 2.0 to test the sensitivity but we found the impact on our simulations to remain relatively small even in the higher flux case.

The stratospheric $\Delta^{17}O$ isoflux follows from the TM5-calculated transfer of air into the troposphere, after we apply a fixed isotope signature of 2.76‰ for $\Delta^{17}O$ in $CO_2$ in the top 5 levels (20–50 km) of TM5. This was chosen to obtain a good match with the global surface abundances and stratospheric isoflux of $\Delta^{17}O$ reported in Hoag et al. (2005) and in our 1D model. This value is also in good agreement with experimental data sampled at the height of 20 km altitude (Boering et al., 2004). Key fluxes and parameters in TM5 are compared to those of the global box model in Table 6.

For all our simulations, we used a vertical resolution of 25 sigma-hybrid levels and a horizontal resolution of $6 \times 4°$ (longitude × latitude). All observational data from Göttingen and Mt. Broken are compared to the model output for a $6 \times 4°$ grid cell that encompasses the Göttingen sampling location. This 3-D framework for $\Delta^{17}O$ is currently being further developed and validated, and fully documented in Schneider (2015).

Table 5
Input parameters for the Monte Carlo simulation.

| Parameter | Mean | SD | Min | Max | Units | References |
|---|---|---|---|---|---|---|
| *GPP* | 120 | 30 | 100 | 180 | PgC/yr | Beer et al. (2010), Welp et al. (2011) |
| $C_{CS}/C_a$ | 0.70 | 0.13 | 0.56 | 0.77 | – | Ciais et al. (1997), Cuntz et al. (2003a), Welp et al. (2011) |
| $\Theta$ | 0.8 | 0.1 | 0.6 | 1 | – | Gillon and Yakir (2000, 2001) |
| $\alpha_L$ | 0.9926 | 0.0030 | 0.9912 | 0.9941 | – | Farquhar et al. (1993) |
| $\alpha_S$ | 0.9928 | 0.0030 | 0.9912 | 0.9941 | – | Miller et al. (1999) |
| $T_{soil}$ | 288 | 2 | 285 | 293 | K | Ciais et al. (1997), Cuntz et al. (2003b) |
| $T_{leaf}$ | 291 | 2 | 286 | 296 | K | Ciais et al. (1997), Cuntz et al. (2003b) |
| $T_{ocean}$ | 291 | 2 | 286 | 296 | K | Ciais et al. (1997), Cuntz et al. (2003b) |
| $\delta_{SW}$ | −7.5 | 3 | −9 | 0 | ‰ | Ciais et al. (1997), Cuntz et al. (2003b) |
| $\alpha_{transpiration}$ | 0.9917 | 0.0010 | 0.9900 | 0.9940 | – | West et al. (2008) |
| $h$ | 0.8 | 0.1 | 0.6 | 1 | – | Ciais et al. (1997) |
| $\theta_{CO_2\text{-water}}$ | 0.5229 | 0.0001 | 0.50 | 0.53 | – | Barkan and Luz (2012) |
| $\lambda_{kinetic}$ | 0.509 | 0.001 | 0.50 | 0.53 | – | Young et al. (2002) |
| $F_{OA}$ | 90 | 10 | 70 | 100 | PgC/yr | Naegler et al. (2006) |
| $F_{SA}$ | 100 | 30 | 25 | 175 | PgC/yr | Appenzeller et al. (1996) |
| $F_{SI}$ | 30 | 120 | 0 | 450 | PgC/yr | Wingate et al. (2009) |

## 5. MODELING RESULTS

### 5.1. Global mass balance of $\Delta^{17}O(CO_2)$

The effect of the various carbon sources and sinks on the global triple oxygen isotope composition of tropospheric $CO_2$ is best illustrated by comparing the $\delta^{18}O$ and $\Delta^{17}O$ isofluxes from our global box model (Fig. 3). The $\delta^{18}O$ isofluxes of the mass balance box model were chosen in accordance with previous modeling studies (see e.g. Ciais et al., 2005). In doing so, the $^{18}O/^{16}O$ ratio of tropospheric $CO_2$ is mainly controlled by assimilation and respiration but the range for the assimilation and respiration isoflux was slightly extended compared to the ranges given by Ciais et al. (2005), see Fig. 3a. This is mainly due to the large variation in the $CO_2$ concentration gradient between chloroplasts and atmosphere ($0.56 < C_{cs}/C_a < 0.77$) and in the terrestrial gross primary production ($100\ PgC/yr < GPP < 180\ PgC/yr$) that were considered for the Monte Carlo simulation.

It is well known that stratospheric $CO_2$ is enriched in $^{18}O$ relative to tropospheric $CO_2$, and as a consequence, the influx of stratospheric $CO_2$ must go along with a positive $\delta^{18}O$ isoflux. In general, $\delta^{18}O$ modeling studies neglect the influx of stratospheric $CO_2$ because the isotopic effect is small (Cuntz et al., 2003a,b; Welp et al., 2011). Here, we consider the estimate of stratospheric $CO_2$ influx from Kawagucci et al. (2008) and conclude that stratospheric $CO_2$ influx indeed does not have a significant impact on the $\delta^{18}O$ composition of tropospheric $CO_2$ (see Fig. 3a).

For the soil invasion flux, we considered findings from Wingate et al. (2009) that the abiotic $CO_2$ flux from soils might have a much larger effect on the oxygen isotope composition of tropospheric $CO_2$ than previously assumed ($0\ PgC/yr < F_{SI} < 450\ PgC/yr$).

The large scatter in $\delta^{18}O$ isofluxes illustrates that modeling the $\delta^{18}O$ value of tropospheric $CO_2$ is very sensitive to various assumptions. Thus, comprehensive bio- and atmosphere models are required to simulate spatial and temporal variations in $\delta^{18}O$ of tropospheric $CO_2$ (Ciais et al., 1997; Cuntz et al., 2003a,b; Welp et al., 2011). As a result, Hoag et al. (2005) suggested that $\Delta^{17}O$ of tropospheric $CO_2$ might be a more straightforward tracer of variations in assimilation and respiration.

The $\Delta^{17}O$ isofluxes from our global box model suggest that the $\Delta^{17}O$ value of tropospheric $CO_2$ is mainly controlled by terrestrial assimilation, respiration, stratospheric influx and soil invasion (see 3b). However, in contrast to the previous $\Delta^{17}O$ model from Hoag et al. (2005), assimilation has a negative effect on $\Delta^{17}O$ of tropospheric $CO_2$, whereas both respiratory $CO_2$ and stratospheric influx have a positive effect on $\Delta^{17}O$ of tropospheric $CO_2$. The negative $\Delta^{17}O$ isoflux for assimilation is mainly a result of kinetic fractionation during $CO_2$ diffusion into the stomata where the diffusional component becomes only relevant for the $CO_2$ fraction that is assimilated by the plant. The effect of evapotranspiration that lowers the $\Delta^{17}O$ signal of the leaf water decreases the negative $\Delta^{17}O$ isoflux only by about 10%. The positive effect of respiratory $CO_2$ on the $\Delta^{17}O$ composition of tropospheric $CO_2$ results from the kinetic fractionation during diffusion out of the soil column assuming a slope $\lambda_{kinetic} = 0.509$ (see Fig. 2). So far, the effect of diffusion on the triple oxygen isotope fractionation during assimilation and respiration has not been determined experimentally but our model assumptions are highly likely within the framework of triple oxygen isotope fractionation.

For the stratospheric $CO_2$ influx, we combine the estimates from Boering et al. (2004) and Kawagucci et al. (2008) on the $^{17}O$ enrichment of stratospheric $CO_2$ influx, and thus, we obtain a slightly higher $\Delta^{17}O$ isoflux for strato-

Table 6
Comparison of fluxes, vegetation parameters, and isofluxes (*IF*) between the one-box model and the TM5 3-D model implementation of the $\Delta^{17}O$ budget. Note that temporal and spatial averaging of $C_i/C_a$ over the 6x4 grid boxes in the TM5 model is based on *GPP* weighted values.

| Parameter | Global mass balance model | TM5/SIBCASA |
|---|---|---|
| $\Delta^{17}O$ atmosphere (‰) | 0.063 | 0.073 |
| *GPP* $C_3$ (PgC/yr) | 92.4 | 93.1 |
| *GPP* $C_4$ (PgC/yr) | 27.6 | 39.9 |
| Total *GPP* | 120 | 133 |
| *TER* (PgC/yr) | 98 | 129 |
| $F_{ff}$ (PgC/yr) | 8 | 9.1 |
| $F_{fire}$ (PgC/yr) | 1 | 1.7 |
| $F_{soil}$ (PgC/yr) | 30 | 38.7 |
| $F_{ocean}$ (PgC/yr) | −2 | −2.99 |
| $C_i/C_a$ (global mean) | 0.7 | 0.74 |
| $C_i/C_a$ ($C_3$, *GPP* weighted) | – | 0.80 |
| $C_i/C_a$ ($C_4$, *GPP* weighted) | – | 0.51 |
| $IF_{AL}$ (PgC‰/yr) | −36.3 | −50.6 |
| $IF_{LA\_eq}$ (PgC‰/yr) | −5.1 | −5.0 |
| $IF_{LA\_noneq}$ (PgC‰/yr) | 5.1 | 7.4 |
| $IF_{resp}$ (PgC‰/yr) | 3.3 | 3.8 |
| $IF_{soil}$ (PgC‰/yr) | −2.1 | −3.6 |
| $IF_{SA}$ (PgC‰/yr) | 44.5 | 39.3 |
| $IF_{ocean}$ (PgC‰/yr) | −6.1 | 0.0 |

spheric $CO_2$ compared to the previous $\Delta^{17}O$ model from Hoag et al. (2005). The assumption on the size of the soil invasion flux also has a considerable effect on the modeled $\Delta^{17}O$ value, whereas fossil fuel emissions and biomass burning do not have a significant impact on the $\Delta^{17}O$ composition of global tropospheric $CO_2$.

### 5.2. Average triple oxygen isotope composition of tropospheric $CO_2$

The mass balance calculation and the Monte Carlo simulation give a global annual mean of tropospheric $CO_2$ of $\Delta^{17}O = +0.061‰ \pm 0.033‰$ (SD). The model prediction confirms the former prediction for the global troposphere from Hoag et al. (2005) with $\Delta^{17}O \approx +0.07‰$ (relative to a reference line with a slope of 0.5229 in a ln $(\delta^{18}O + 1)$ vs. ln $(\delta^{17}O + 1)$ plot). The tracer transport model TM5 predicts a global tropospheric mean surface value of $+0.08 \pm 0.02‰$, in close agreement with the box model formulation it is derived from. For the grid box of Göttingen, the TM5 model results in a slightly lower $\Delta^{17}O$ value of $+0.04 \pm 0.01‰$ (SD) due to the higher biospheric activity compared to the global average.

The measured $\Delta^{17}O$ values for tropospheric carbon dioxide sampled in Göttingen vary between $-0.21‰$ and $+0.07‰$ with an average value of $-0.07 \pm 0.05‰$ (SD) (Fig. 1, Table 1). As mentioned, the triple oxygen isotope composition observed in the first year ($-0.02 \pm 0.05‰$ (SD)) is significantly higher than the one observed in the second year ($-0.12 \pm 0.04‰$ (SD)), and the second year of our measurements would not encompass the Göttingen-specific or globally simulated $\Delta^{17}O$ within its 68% confidence interval.

For the $\delta^{18}O$ mass balance calculation, the base scenario (see Tables 3 and 4) results in $\delta^{18}O = 41.3‰$ and the Monte Carlo simulation (see Table 5) in $\delta^{18}O = 40.9 \pm 1.9‰$ (SD). The modeled mean $\delta^{18}O$ value is in good agreement with the observed global mean of about 41.5‰ (e.g. Farquhar et al., 1993). The large uncertainty in the $\delta^{18}O$ model prediction gives a very conservative estimate for the global troposphere, in order to test the maximum effect of the model assumptions on the $\Delta^{17}O$ prediction of tropospheric $CO_2$.

### 5.3. The simulated seasonal cycle of $\Delta^{17}O(CO_2)$ at Göttingen

We show the atmospheric $\Delta^{17}O$ values simulated with the 3-D modeling framework for the Göttingen grid box in Figs. 4 and 5. The modeled seasonal variation has an amplitude of about 0.05‰ and is dominated by the seasonal variations in the biosphere (see Fig. 5b). Contributions from stratospheric sources, soil invasion, and fossil fuel fluxes are minor terms that contribute to, but do not dominate the seasonal cycle.

High assimilation rates during spring and summer cause a strong negative isoflux for the carbon uptake flux (atmosphere-leaf flux) with most negative isoflux values in June (Fig. 5, also see Section 5.2). The modeled minimum values in $\Delta^{17}O$ of tropospheric $CO_2$ occur after the summer (October) and lag the maximum of the surface fluxes (June/July) by about three months (Figs. 4 and 5). This minimum is attained in autumn because the sum of the isofluxes continues to deplete the atmosphere in $\Delta^{17}O$ until *GPP* becomes too small to compensate for stratospheric supply of high $\Delta^{17}O$ air.

A direct comparison between the modeled and observed seasonality is impeded by the large drop in the observed $\Delta^{17}O(CO_2)$ signal in late summer 2011. In order to focus on the seasonality, we force the mean value of the model to be zero and compare it to the observed, detrended $\Delta^{17}O(CO_2)$ time series (Fig. 4b). We find that the phasing of the modeled seasonality agrees well with the observed one but the modeled amplitude is about a factor three smaller.

A secondary minimum in observed $\Delta^{17}O$ occurs in January/February in both years, but is not reproduced by the model. From the shape of the isofluxes a possible late-winter low in stratospheric inflow could have contributed, but its modeled amplitude is too small to explain the observations. Further attempts to increase the seasonal amplitude of the model by increasing soil invasion fluxes of $CO_2$ (up to 260 PgC/yr), and by decreasing the average leaf-water $\Delta^{17}O$ value, did not substantially alter the seasonal cycle amplitude, and therefore did not improve our match to observations.

## 6. DISCUSSION

### 6.1. Comparison to literature data on $\Delta^{17}O(CO_2)$ in the lower atmosphere

Literature data on the triple oxygen isotope composition of tropospheric $CO_2$ are scarce (see Fig. 6). Barkan and Luz (2012) were the first to report high precision data on the triple oxygen isotope composition of tropospheric $CO_2$. They found a $\Delta^{17}O$ value of $+0.037 \pm 0.009‰$ (SD, relative to $\lambda_{RL} = 0.5229$) for a limited set of tropospheric $CO_2$ sampled in spring 2012 in Jerusalem (Israel). Thiemens et al. (2014) report a decadal record of $\Delta^{17}O$ values of tropospheric $CO_2$ sampled in La Jolla, California (USA). They observed a mean $\Delta^{17}O$ value of $+0.03 \pm 0.04‰$ (relative to $\lambda_{RL} = 0.5229$) and proposed that this mean value reflects a stratospheric component in the troposphere. Liang and Mahata (2015) report a six months $\Delta^{17}O$ record of near-surface $CO_2$ sampled in Taiwan and they observed on average a $\Delta^{17}O$ value of $+0.06 \pm 0.04‰$ (relative to $\lambda_{RL} = 0.5229$). These studies are in excellent agreement with the revised model prediction for the global troposphere ($\Delta^{17}O = +0.06 \pm 0.03‰$ (SD)) and the $\Delta^{17}O$ values observed during the first year in this study ($-0.02 \pm 0.05‰$ (SD)) (see Fig 6).

### 6.2. On the year-to-year variations in $\Delta^{17}O(CO_2)$

The observed $\Delta^{17}O(CO_2)$ values decrease by about $-0.1‰$ from the first year (2010/2011) to the second year (2011/2012) and in the absence of evidence of a measurement bias, we speculate on its cause. An interannual drop in $\Delta^{17}O$ of tropospheric $CO_2$ may be caused by a decrease in influx of mass-independently fractionated stratospheric $CO_2$, an increase in biospheric activity or an increase in

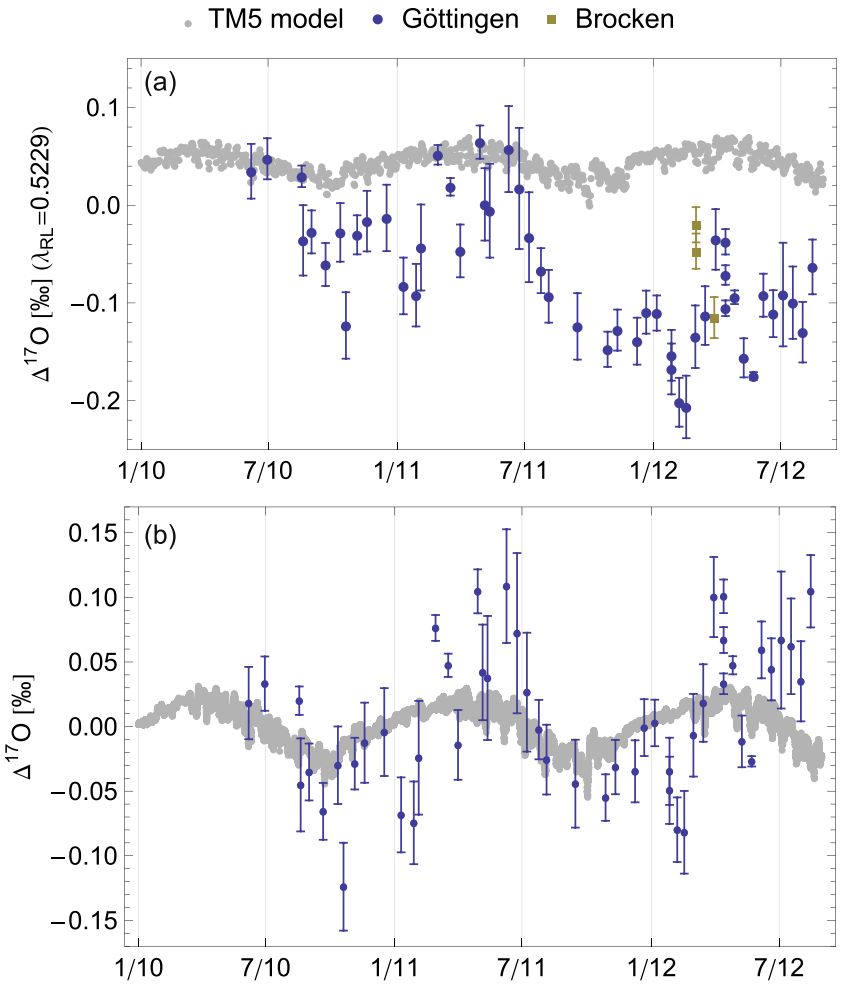


Fig. 4. Comparison between observed (see Section 3.2) and modeled (see Section 5) temporal variation of the triple oxygen isotope composition of tropospheric $CO_2$ for Göttingen (Germany). (a) Uncorrected observational and TM5 model data. The mass balance assumptions for $\Delta^{17}O$ of tropospheric $CO_2$ were combined with the SiBCASA terrestrial biosphere model and the global 3D transport model TM5 in order to determine the $\Delta^{17}O$ (trop. $CO_2$) variations for a $1° \times 1°$ grid box enclosing the sampling location. The simulated seasonal variation of $\Delta^{17}O$ is largely the result of seasonal variations in plant activity. The daily variations in the simulation data are due to variability in biospheric activity as well as variations in the atmospheric boundary layer. The modeled and observed $\Delta^{17}O$ ($CO_2$) data from the second year deviate by about −0.2‰. The reason for this large discrepancy is unclear. (b) Intra-annual variation of $\Delta^{17}O$ ($CO_2$): Detrended simulation and detrended observational data. The phasing between model and observational data agrees well: The observational data show an amplitude of 0.11‰ in the first year (2010/2011) and 0.14‰ in the second year (2011/2012). The modeled seasonal variation is less distinct (about 0.045‰ in both years). The observational data peak in June/July and the simulation data peak about three months earlier in March/April.

anthropogenic $CO_2$ emissions (see Fig. 3). Due to the distinct enrichment of stratospheric $CO_2$ in $^{17}O$ (Boering et al., 2004; Kawagucci et al., 2008), variations in stratospheric $CO_2$ influx may affect the triple oxygen isotope composition significantly (Liang and Mahata, 2015). However, our global box-model requires unrealistically large decreases in stratosphere-troposphere exchange to reproduce the large interannual $\Delta^{17}O$ drop observed in Göttingen (i.e. only the complete absence of stratospheric signal would result in a 0.1‰ drop within five years). Variations in biospheric activity can also affect the triple oxygen isotope composition (see Section 5.1), but again, it requires an unrealistically large increase in gross primary production to account for the interannual drop in $\Delta^{17}O$ (i.e. a *GPP* anomaly of 2500 PgC/yr is needed to model a drop in $\Delta^{17}O$ by 0.1‰ within one year).

Finally, elevated anthropogenic $CO_2$ emissions may lower the $\Delta^{17}O$ value of tropospheric $CO_2$ because they can inherit a distinct triple oxygen isotope composition from ambient air $O_2$ (Horváth et al., 2012). During the two-year sampling period we observed $CO_2$ concentrations that were up to 75 ppm higher than the background level (Fig. 1a). To test the hypothesis that elevated anthropogenic carbon dioxide levels have had a strong impact on our observed $\Delta^{17}O$ time series, we performed a separate TM5 simulation in which we assumed that carbon dioxide

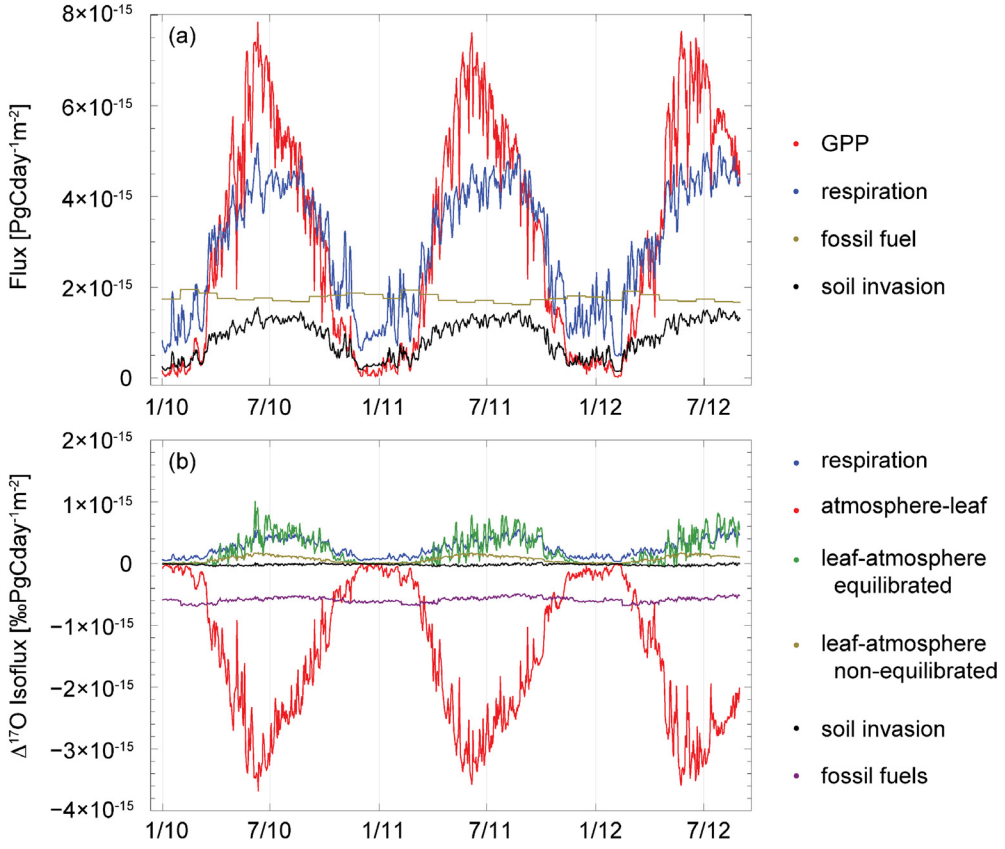


Fig. 5. (a) Seasonal variation of carbon fluxes in the Göttingen area. The fluxes for the biosphere were derived from the SiBCASA biosphere model. (b) $\Delta^{17}O$ isofluxes for Göttingen. Variations in the atmosphere-leaf flux show the strongest seasonality.

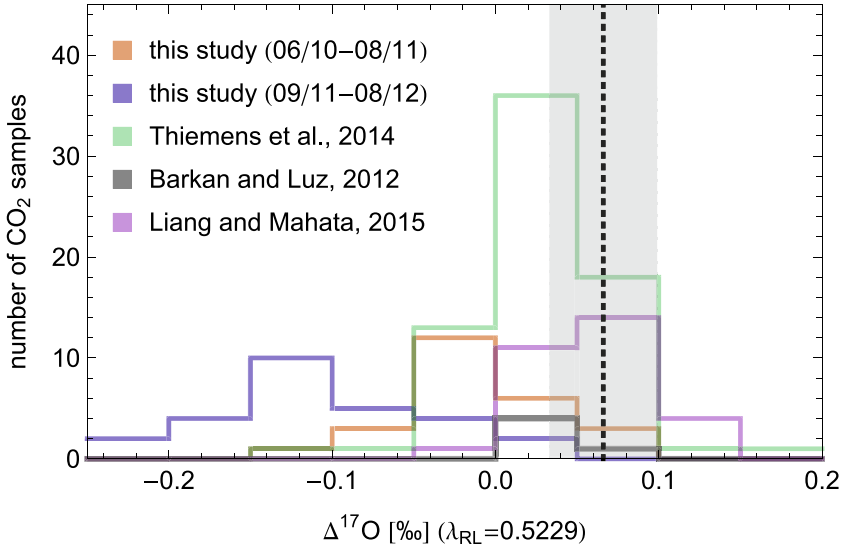


Fig. 6. Comparison between the mass balance model prediction for the global troposphere (dashed line with gray error envelope) and observational data: Göttingen (this study), California/US (Thiemens et al., 2014, sampled 1990–2000), Taipei/Taiwan (Liang and Mahata, 2015, sampled 2013/2014) and Jerusalem, Israel (Barkan and Luz, 2012, sampled 2012). The literature data were converted to a reference line of 0.5229.

concentrations above the background level were solely due to a combustion-derived $CO_2$ and calculated a correction term for the $\Delta^{17}O$ time series data accordingly. This correction term could not explain the discrepancy between the simulated time series and the observed one and had a maximum impact of 0.025‰ during the winter months. Thus,

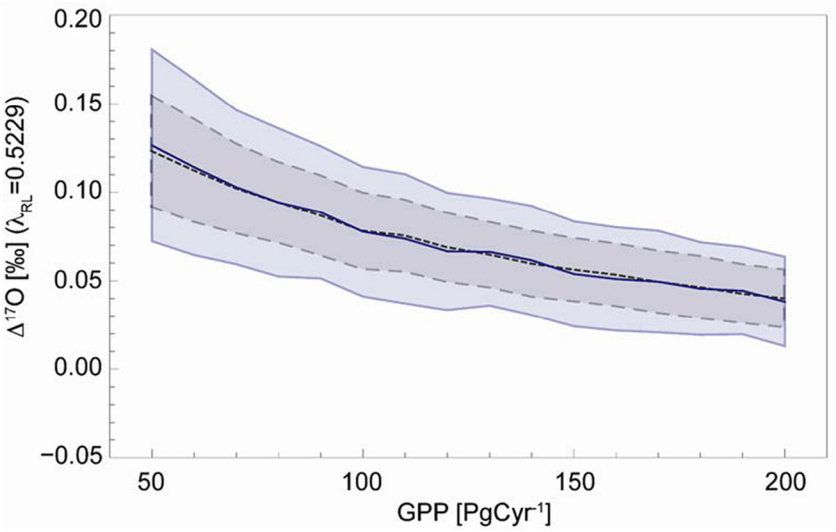


Fig. 7. Modeled sensitivity of $\Delta^{17}O$ of tropospheric $CO_2$ to variations in the terrestrial gross primary production (*GPP*). The solid line and the corresponding error envelope show the result from the Monte Carlo simulation including the uncertainty of all model parameters (see Table 5). The dashed line and its corresponding error envelope show the sensitivity simulation assuming no uncertainty in stratospheric influx. The error envelopes denote the standard deviation obtained from the Monte Carlo simulation.

although ambient air $CO_2$ from Göttingen could be strongly affected by local anthropogenic $CO_2$ emissions, these cannot account for the interannual variation nor the seasonal variation in the triple oxygen isotope composition. This is further supported by the fact that the Mt. Brocken $CO_2$ data with $CO_2$ concentrations close to background level fall within the range observed in Göttingen ($-0.05 \pm 0.02$‰ (SE), $-0.02 \pm 0.02$‰ (SE) and $-0.12 \pm 0.02$‰ (SE).

This leaves the year-to-year change unexplained for the moment, calling for more observations at non-background locations. However, we note that Thiemens et al. (2014) also observed a year-to-year drop in $\Delta^{17}O$ of $CO_2$ sampled in La Jolla, California of about 0.06‰ in their decadal time series. The authors assume that an increase in *GPP* due to an ENSO event in 1997–1999 might have caused this drop, and mention possible variations in the stratosphere-troposphere exchange. Our current model cannot quantitatively verify the ENSO hypothesis, but does not support a large year-to-year change in stratospheric $\Delta^{17}O$ near the surface. In our opinion, the observed year-to-year variations in $\Delta^{17}O$ of tropospheric $CO_2$ illustrate that its budget is not yet fully understood.

### 6.3. Is $\Delta^{17}O$ of tropospheric $CO_2$ a potential tracer for the terrestrial gross primary production?

We tested the sensitivity of $\Delta^{17}O$ of global tropospheric $CO_2$ to *GPP*. The mass balance model predicts that a 3-fold change from 50 to 150 PgC/yr results in a $\Delta^{17}O$ decrease of about $-0.08$‰ (Fig. 7). This sensitivity to *GPP* is slightly lower than the prediction of $-0.11$‰ for a decrease from 50 to 150 PgC/yr from Hoag et al. (2005). Thus, the revised global mass balance box model confirms that $\Delta^{17}O$ of tropospheric $CO_2$ is a potential tracer for the activity of the terrestrial biosphere. However, the Monte Carlo simulation shows that this sensitivity to *GPP* can be masked by the uncertainty of other model parameters, mainly the uncertainty in stratospheric $CO_2$ influx (see Fig. 7). Thus, in order to use $\Delta^{17}O$ of $CO_2$ as a tracer for *GPP* better constrains for the parameters listed in Table 5 are required and a measurement precision of 0.01‰ or better should be achieved.

This study shows that the triple oxygen isotope composition of tropospheric $CO_2$ captures the seasonal variability of gross primary productivity. Thus, our observational data in combination with the new three-dimensional transport model confirm the hypothesis from Hoag et al. (2005) that $\Delta^{17}O$ is a tracer of biospheric activity. The new $\Delta^{17}O$ framework in combination with the TM5 model provides the basis for the interpretation of spatiotemporal variations in $\Delta^{17}O$ of tropospheric $CO_2$. However, not all aspects of the observed temporal $\Delta^{17}O$ variation are captured in the simulation.

We suggest that the effect of assimilation and respiration on $\Delta^{17}O$ of tropospheric $CO_2$ should be determined experimentally and we plan to implement photolytic reaction mechanisms into the TM5 model to simulate the stratospheric component more explicitly. Ultimately, more $\Delta^{17}O$ measurements of tropospheric $CO_2$ at background locations are needed to validate the model.

## 7. CONCLUSION

- A revised mass balance calculation for tropospheric carbon dioxide combined with a Monte Carlo simulation predicts that the global average $\Delta^{17}O$ value is $+0.06$‰ $\pm 0.03$‰ (SD) (relative to a reference slope of 0.5229).

This prediction confirms the former prediction from Hoag et al. (2005) (+0.07‰ relative to a reference slope of 0.5229).

- Tropospheric $CO_2$ sampled in Göttingen in 2010/2011 has a $\Delta^{17}O$ value of $-0.02 \pm 0.05$‰ (SD). The data overlap with the TM5 model simulation for a $1 \times 1°$ grid box surrounding Göttingen ($\Delta^{17}O = +0.044 \pm 0.012$‰). Literature data observed in tropospheric air in La Jolla, California ($+0.03 \pm 0.04$‰) (Thiemens et al., 2014), Jerusalem, Israel ($+0.037 \pm 0.009$‰ (SD)) (Barkan and Luz, 2012) and Taipei, Taiwan ($+0.06 \pm 0.04$‰ (SD)) (Liang and Mahata, 2015) agree well with the 2010/2011 observation in Göttingen and the prediction for the global troposphere ($+0.06 \pm 0.05$‰). The carbon dioxide sampled in 2011/2012 shows a significantly lower $\Delta^{17}O$ value of $-0.12 \pm 0.04$‰ (SD). The reason for this inter-annual drop is unclear.
- The model calculation confirm that $\Delta^{17}O$ of tropospheric $CO_2$ is sensitive to the gross primary productivity. A 3-fold change in *GPP* from 50 to 150 PgC/yr induced a decrease in $\Delta^{17}O$ of about $-0.08$‰. But in order to exploit this new tracer for *GPP* other model parameters have to be refined (notably the influx of stratospheric air) and an even higher measurement precision is required.
- The $\Delta^{17}O$ time series of tropospheric air sampled in Göttingen shows a pronounced seasonal cycle with an amplitude (peak-to-trough) of about $0.13 \pm 0.02$‰ (SD). The simulation of the $\Delta^{17}O$ of tropospheric $CO_2$ in Göttingen shows that the seasonal variations can be traced back to seasonal variations in assimilation. This first observation of a seasonal cycle in $\Delta^{17}O$ of tropospheric $CO_2$ illustrates its potential use as a tracer for terrestrial biospheric activity.

## ACKNOWLEDGMENT

We thank M. Cuntz and J. Kaiser for very helpful comments on the mass balance calculation and E. Barkan for calibration of our inhouse reference $O_2$ gas relative to VSMOW. We also thank M. Troche, N. Albrecht, A. Gehler and R. Przybilla for their help in the laboratory. This project was partly funded by the German Science Foundation (AP, project PA909/6-2).

## APPENDIX A. SUPPLEMENTARY DATA

Supplementary data associated with this article can be found, in the online version, at http://dx.doi.org/10.1016/j.gca.2016.11.019.

## REFERENCES

Appenzeller C., Holton J. R. and Rosenlof K. H. (1996) Seasonal variation of mass transport across the tropopause. *J. Geophys. Res.* **101**, 15071–15078.

Assonov S. S., Brenninkmeijer C. A. M., Koeppel C. and Röckmann T. (2009) $CO_2$ isotope analyses using large air samples collected on intercontinental flights by the CARIBIC Boeing 767. *Rapid Commun. Mass Spectrom.* **23**, 822–830.

Barkan E. and Luz B. (2011) The relationships among the three stable isotopes of oxygen in air, seawater and marine photosynthesis. *Rapid Commun. Mass Spectrom.* **25**, 2367–2369.

Barkan E. and Luz B. (2012) High-precision measurements of $^{17}O/^{16}O$ and $^{18}O/^{16}O$ ratios in $CO_2$. *Rapid Commun. Mass Spectrom.* **26**, 2733–2738.

Beer C., Reichstein M., Tomelleri E., Ciais P., Jung M., Carvalhais N., Rödenbeck C., Arain M. A., Baldocchi D., Bonan G. B., Bondeau A., Cescatti A., Lasslop G., Lindroth A., Lomas M., Luyssaert S., Margolis H., Oleson K. W., Roupsard O., Veenendaal E., Viovy N., Williams C., Woodward F. I. and Papale D. (2010) Terrestrial gross carbon dioxide uptake: global distribution and covariation with climate. *Science* **329**, 834–838.

Boden, T.A., G. Marland, and R.J. Andres. 2011. Global, Regional, and National Fossil-Fuel $CO_2$ Emissions. Carbon Dioxide Information Analysis Center, Oak Ridge National Laboratory, U.S. Department of Energy, Oak Ridge, Tenn., U. S.A. http://dx.doi.org/10.3334/CDIAC/00001_V2011.

Boering K. A., Jackson T., Hoag K. J., Cole A. S., Perri M. J., Thiemens M. and Atlas E. (2004) Observations of the anomalous oxygen isotopic composition of carbon dioxide in the lower stratosphere and the flux of the anomaly to the troposphere. *Geophys. Res. Lett.* **31**.

Brenninkmeijer C. A. M. (1991) Robust, high-efficiency, high-capacity cryogenic trap. *Anal. Chem.* **63**, 1182–1184.

Brenninkmeijer C. A. M. and Röckmann T. (1996) Russian doll type cryogenic traps: improved design and isotope separation effects. *Anal. Chem.* **68**, 3050–3053.

Brenninkmeijer C. A. M., Kraft P. and Mook W. G. (1983) Oxygen isotope fractionation between $CO_2$ and $H_2O$. *Isot. Geosci.* **1**, 181–190.

Brugnoli E., Hubick K. T., von Caemmerer S., Wong S. C. and Farquhar G. D. (1988) Correlation between the carbon isotope discrimination in leaf starch and sugars of $C_3$ plants and the ratio of intercellular and atmospheric partial pressures of carbon dioxide. *Plant Physiol.* **88**, 1418–1424.

Canadell J. G., Le Quéré C., Raupach M. R., Field C. B., Buitenhuis E. T., Ciais P., Conway T. J., Gillett N. P., Houghton R. A. and Marland G. (2007) Contributions to accelerating atmospheric $CO_2$ growth from economic activity, carbon intensity, and efficiency of natural sinks. *Proc. Natl. Acad. Sci.* **104**, 18866–18870.

Ciais P., Tans P. P., Trolier M., White J. W. C. and Francey R. J. (1995) A large northern hemisphere terrestrial $CO_2$ sink indicated by the $^{13}C/^{12}C$ ratio of atmospheric $CO_2$. *Science* **269**, 1098–1102.

Ciais P., Denning A. S., Tans P. P., Berry J. A., Randall D., Collatz J. G., Sellers P. J., White J. W., Trolier M., Meijer H. A. J., Francey R. J., Monfray P. and Heimann M. (1997) A three-dimensional synthesis study of $\delta^{18}O$ in atmospheric $CO_2$: part 1 Surface fluxes. *J. Geophys. Res.* **102**, 5857–5872.

Ciais P., Cuntz M., Scholze M., Mouillot F., Peylin P. and Gitz V. (2005) Remarks on the use of $^{13}C$ and $^{18}O$ isotopes in atmospheric $CO_2$ to quantify biospheric carbon fluxes. In *Stable Isotopes and Biosphere – Atmosphere Interactions: processes and Biological Controls* (eds. L. B. Flanagan, J. R. Ehleringer, and D. E. Pataki). Elsevier. pp. 235–267.

Cuntz M., Ciais P., Hoffmann G., Allison C. E., Francey R. J., Knorr W., Tans P. P., White J. W. C. and Levin I. (2003a) A comprehensive global three-dimensional model of $\delta^{18}O$ in atmospheric $CO_2$: 2. Mapping the atmospheric signal. *J. Geophys. Res.* **108**. ACH2.1-ACH2.19.

Cuntz M., Ciais P., Hoffmann G. and Knorr W. (2003b) A comprehensive global three-dimensional model of $\delta^{18}O$ in atmospheric $CO_2$: 1. Validation of surface processes. *J. Geophys. Res.* **108**. ACH1-ACH23.

Farquhar G. D., Lloyd J., Taylor J. A., Flanagan L. B., Syvertsen J. P., Hubick K. T., Wong S. C. and Ehleringer J. R. (1993) Vegetation effects on the isotope composition of oxygen in atmospheric $CO_2$. *Nature* **363**, 439–443.

Gamo T., Tsutsumi M., Sakai H., Nakazawa T., Tanaka M., Honda H., Kubo H. and Itoh T. (1989) Carbon and oxygen isotopic ratios of carbon dioxide of a stratospheric profile over Japan. *Tellus* **B41B**, 127–133.

Gillon J. S. and Yakir D. (2000) Naturally low carbonic anhydrase activity in $C_4$ and $C_3$ plants limits discrimination against $C^{18}OO$ during photosynthesis. *Plant, Cell Environ.* **23**, 903–915.

Gillon J. and Yakir D. (2001) Influence of carbonic anhydrase activity in terrestrial vegetation on the $^{18}O$ content of atmospheric $CO_2$. *Science* **291**, 2584–2587.

Gehler A., Gingerich P. D. and Pack A. (2016) Temperature and atmospheric $CO_2$ concentration estimates through the PETM using triple oxygen isotope analysis of mammalian bioapatite. *Proc. Natl. Acad. Sci.* **113**, 7739–7744.

Guy R. D., Fogel M. L. and Berry J. A. (1993) Photosynthetic fractionation of the stable isotopes of oxygen and carbon. *Plant Physiol.* **101**, 37–47.

Heimann M. and Maier-Reimer E. (1996) On the relations between the oceanic uptake of $CO_2$ and its carbon isotopes. *Global Biogeochem. Cycles* **10**, 89–110.

Herwartz D., Pack A., Friedrichs B. and Bischoff A. (2014) Identification of the giant impactor Theia in lunar rocks. *Science* **344**, 1146–1150.

Hoag K. J., Still C. J., Fung I. Y. and Boering K. A. (2005) Triple oxygen isotope composition of tropospheric carbon dioxide as a tracer of terrestrial gross carbon fluxes. *Geophys. Res. Lett.* **32**, 1–5.

Hofmann M. E. G. and Pack A. (2010) Technique for high-precision analysis of triple oxygen isotope ratios in carbon dioxide. *Anal. Chem.* **82**, 4357–4361.

Hofmann M. E. G., Horváth B. and Pack A. (2012) Triple oxygen isotope equilibrium fractionation between carbon dioxide and water. *Earth Planet. Sci. Lett.* **319–320**, 159–164.

Horváth B., Hofmann M. E. G. and Pack A. (2012) On the triple oxygen isotope composition of carbon dioxide from some combustion processes. *Geochim. Cosmochim. Acta* **95**, 160–168.

Huijnen V., Williams J., van Weele M., van Noije T., Krol M., Dentener F., Segers A., Houweling S., Peters W., de Laat J., Boersma F., Bergamaschi P., van Velthoven P., Le Sager P., Eskes H., Alkemade F., Scheele R., Nédélec P. and Pätz H.-W. (2010) The global chemistry transport model TM5: description and evaluation of the tropospheric chemistry version 3.0. *Geosci. Model Dev.* **3**, 445–473.

Hulston J. R. and Thode H. G. (1965) Variations in the $S^{33}$, $S^{34}$, and $S^{36}$ contents of meteorites and their relation to chemical and nuclear effects. *J. Geophys. Res.* **70**, 3475–3484.

Kaiser J. (2008) Reformulated $^{17}O$ correction of mass spectrometric stable isotope measurements in carbon dioxide and a critical appraisal of historic "absolute" carbon and oxygen isotope ratios. *Geochim. Cosmochim. Acta* **72**, 1312–1334.

Kawagucci S., Tsunogai U., Kudo S., Nakagawa F., Honda H., Aoki S., Nakazawa T., Tsutsumi M. and Gamo T. (2008) Long-term observation of mass-independent oxygen isotope anomaly in stratospheric $CO_2$. *Atmos. Chem. Phys.* **8**, 6189–6197.

Kim S.-T., Mucci A. and Taylor B. E. (2007) Phosphoric acid fractionation factors for calcite and aragonite between 25 and 75 °C: Revisited. *Chem. Geol.* **246**, 135–146.

Krol M., Peters W., Hooghiemstra P., George M., Clerbaux C., Hurtmans D., McInerney D., Sedano F., Bergamaschi P., El Hajj M., Kaiser J. W., Fisher D., Yershov V. and Muller J.-P. (2013) How much CO was emitted by the 2010 fires around Moscow? *Atmos. Chem. Phys.* **13**, 4737–4747.

Lämmerzahl P., Röckmann T., Brenninkmeijer C. A. M., Krankowsky D. and Mauersberger K. (2002) Oxygen isotope composition of stratospheric carbon dioxide. *Geophys. Res. Lett.* **29**, 1582.

Landais A., Barkan E., Yakir D. and Luz B. (2006) The triple isotopic composition of oxygen in leaf water. *Geochim. Cosmochim. Acta* **70**, 4105–4115.

Landais A., Barkan E. and Luz B. (2008) Record of $\delta^{18}O$ and $^{17}O$-excess in ice from Vostok Antarctica during the last 150,000 years. *Geophys. Res. Lett.* **35**.

Le Quéré C., Raupach M. R., Canadell J. G. and Marland G., et al. (2009) Trends in the sources and sinks of carbon dioxide. *Nat. Geosci.* **2**, 831–836.

Le Quéré C., Moriarty R., Andrew R., Peters G., Ciais P., Friedlingstein P., Jones S., Sitch S., Tans P., Arneth A., Boden T., Bopp L., Bozec Y., Canadell J., Chini L., Chevallier F., Cosca C., Harris I., Hoppema M., Houghton R., House J., Jain A., Johannessen T., Kato E., Keeling R., Kitidis V., Klein Goldewijk K., Koven C., Landa C., Landschützer P., Lenton A., Lima I., Marland G., Mathis J., Metzl N., Nojiri Y., Olsen A., Ono T., Peng S., Peters W., Pfeil B., Poulter B., Raupach M., Regnier P., Rödenbeck C., Saito S., Salisbury J., Schuster U., Schwinger J., Séférian R., Segschneider J., Steinhoff T., Stocker B., Sutton A., Takahashi T., Tilbrook B., Van Der Werf G., Viovy N., Wang Y., Wanninkhof R., Wiltshire A. and Zeng N. (2015) Global carbon budget 2014.

Liang M.-C. and Mahata S. (2015) Oxygen anomaly in near surface carbon dioxide reveals deep stratospheric intrusion. *Sci. Rep.* **5**, 11352.

Lloyd J. and Farquhar G. D. (1994) $C^{13}$ discrimination during $CO_2$ assimilation by the terrestrial biosphere. *Oecologia* **99**, 201–215.

Loftfield N., Flessa H., Augustin J. and Beese F. (1997) Automated gas chromatographic system for rapid analysis of the atmospheric trace gases methane, carbon dioxide, and nitrous oxide. *J. Environ. Qual.* **26**, 560.

Luz B. and Barkan E. (2010) Variations of $^{17}O/^{16}O$ and $^{18}O/^{16}O$ in meteoric waters. *Geochim. Cosmochim. Acta* **74**, 6276–6286.

Mahata S., Bhattacharya S. K., Wang C.-H. and Liang M.-C. (2012) An improved $CeO_2$ method for high-precision measurements of $^{17}O/^{16}O$ ratios for atmospheric carbon dioxide. *Rapid Commun. Mass Spectrom.* **26**, 1909–1922.

Mahata S., Bhattacharya S. K., Wang C.-H. and Liang M.-C. (2013) Oxygen isotope exchange between $O_2$ and $CO_2$ over hot platinum: an innovative technique for measuring $\Delta^{17}O$ in $CO_2$. *Anal. Chem.* **85**, 6894–6901.

Meirink J. F., Bergamaschi P. and Krol M. C. (2008) Four-dimensional variational data assimilation for inverse modelling of atmospheric methane emissions: method and comparison with synthesis inversion. *Atmos. Chem. Phys.* **8**, 6341–6353.

Miller M. F. (2002) Isotopic fractionation and the quantification of $^{17}O$ anomalies in the oxygen three-isotope system: an appraisal and geochemical significance. *Geochim. Cosmochim. Acta* **66**, 1881–1889.

Miller J. B., Yakir D., White J. W. C. and Tans P. P. (1999) Measurement of $^{18}O/^{16}O$ in the soil-atmosphere $CO_2$ flux. *Global Biogeochem. Cycles* **13**, 761–774.

Naegler T., Ciais P., Rodgers K. and Levin I. (2006) Excess radiocarbon constraints on air-sea gas exchange and the uptake of $CO_2$ by the oceans. *Geophys. Res. Lett.* **33**, L11802.

Pack A. and Herwartz D. (2014) The triple oxygen isotope composition of the Earth mantle and understanding variations

in terrestrial rocks and minerals. *Earth Planet. Sci. Lett.* **390**, 138–145.

Passey B. H., Hu H., Ji H., Montanari S., Li S., Henkes G. A. and Levin N. E. (2014) Triple oxygen isotopes in biogenic and sedimentary carbonates. *Geochim. Cosmochim. Acta* **141**, 1–25.

Pearcy R. W. and Ehleringer J. (1984) Comparative ecophysiology of $C_3$ and $C_4$ plants. *Plant, Cell Environ.* **7**, 1–13.

Peters W. (2004) Toward regional-scale modeling using the two-way nested global model TM5: characterization of transport using $SF_6$. *J. Geophys. Res.* **109**, D19314.

Peters W., Krol M. C., van der Werf G. R., Houweling S., Jones C. D., Hughes J. H., Schaefer K., Masarie K. A., Jacobson A. R., Miller J. B., Cho C. H., Ramonet M., Schmidt M., Ciattaglia L., Apadula F., Heltai D., Meinhardt F., Di Sarra A. G., Piacentino S., Sferlazzo D., Aalto T., Hatakka J., Ström J., Haszpra L., Meijer H. A. J., Van Der Laan S., Neubert R. E. M., Jordan A., Rodó X., MORGUÍ J.-A., Vermeulen A. T., Popa E., Rozanski K., Zimnoch M., Manning A. C., Leuenberger M., Uglietti C., Dolman A. J., Ciais P., Heimann M. and Tans P. P. (2010) Seven years of recent European net terrestrial carbon dioxide exchange constrained by atmospheric observations. *Glob. Chang. Biol.* **16**, 1317–1337.

Schaefer K., Collatz G. J., Tans P., Denning A. S., Baker I., Berry J., Prihodko L., Suits N. and Philpott A. (2008) Combined Simple Biosphere/Carnegie-Ames-Stanford Approach terrestrial carbon cycle model. *J. Geophys. Res.* **113**, G03034.

Schneider L. (2015) *Simulating the global distribution of $\Delta^{17}O$ in $CO_2$* Master thesis. Wageningen University.

Stern L. A., Amundson R. and Baisden W. T. (2001) Influence of soils on oxygen isotope ratio of atmospheric $CO_2$. *Global Biogeochem. Cycles* **15**, 753–759.

Still C. J., Berry J. A., Collatz G. J. and DeFries R. S. (2003) Global distribution of $C_3$ and $C_4$ vegetation: carbon cycle implications. *Global Biogeochem. Cycles* **17**.

Tans P. P. (1998) Oxygen isotopic equilibrium between carbon dioxide and water in soils. *Tellus B* **50**, 163–178.

Thiemens M. H., Jackson T., Zipf E. C., Erdman P. W. and van Egmond C. (1995) Carbon dioxide and oxygen isotope anomalies in the mesosphere and stratosphere. *Science* **270**, 969–972.

Thiemens M. H., Chakraborty S. and Jackson T. L. (2014) Decadal $\Delta^{17}O$ record of tropospheric $CO_2$: verification of a stratospheric component in the troposphere. *J. Geophys. Res. Atmos.* **119**, 2013JD020317.

Thoning K. W., Tans P. P. and Komhyr W. D. (1989) Atmospheric carbon dioxide at Mauna Loa Observatory: 2. Analysis of the NOAA GMCC data, 1974–1985. *J. Geophys. Res.* **94**, 8549.

West J. B., Sobek A. and Ehleringer J. R. (2008) A simplified GIS approach to modeling global leaf water isoscapes. *PLoS One* **3**, e2447.

van der Velde I. R., Miller J. B., Schaefer K., van der Werf G. R., Krol M. C. and Peters W. (2014) Terrestrial cycling of $^{13}CO_2$ by photosynthesis, respiration, and biomass burning in SiBCASA. *Biogeosciences* **11**, 6553–6571.

van der Werf G. R., Randerson J. T., Collatz G. J., Giglio L., Kasibhatla P. S., Arellano A. F., Olsen S. C. and Kasischke E. S. (2004) Continental-scale partitioning of fire emissions during the 1997 to 2001 El Niño/La Niña period. *Science* **303**, 73–76.

Welp L. R., Keeling R. F., Meijer H. A. J., Bollenbacher A. F., Piper S. C., Yoshimura K., Francey R. J., Allison C. E. and Wahlen M. (2011) Interannual variability in the oxygen isotopes of atmospheric $CO_2$ driven by El Niño. *Nature* **477**, 579–582.

Wiegel A. A., Cole A. S., Hoag K. J., Atlas E. L., Schauffler S. M. and Boering K. A. (2013) Unexpected variations in the triple oxygen isotope composition of stratospheric carbon dioxide. *Proc. Natl. Acad. Sci.* **110**, 17680–17685.

Wingate L., Ogée J., Cuntz M., Genty B., Reiter I., Seibt U., Yakir D., Maseyk K., Pendall E. G., Barbour M. M., Mortazavi B., Burlett R., Peylin P., Miller J., Mencuccini M., Shim J. H., Hunt J. and Grace J. (2009) The impact of soil microorganisms on the global budget of $\delta^{18}O$ in atmospheric $CO_2$. *Proc. Natl. Acad. Sci.* **106**, 22411–22415.

Young E. D., Galy A. and Nagahara H. (2002) Kinetic and equilibrium mass-dependent isotope fractionation laws in nature and their geochemical and cosmochemical significance. *Geochim. Cosmochim. Acta* **66**, 1095–1104.

*Associate editor:* Hagit Affek